# Nerve injury reduces responses of hypoglossal motoneurones to baseline and chemoreceptor-modulated inspiratory drive in the adult rat

David González-Forero, Federico Portillo, Carmen R. Sunico and Bernardo Moreno-López

*Área de Fisiología, Facultad de Medicina, Universidad de Cádiz, Cádiz, Spain*

**The effects of peripheral nerve lesions on the membrane and synaptic properties of motoneurones have been extensively studied. However, minimal information exists about how these alterations finally influence discharge activity and motor output under physiological afferent drive. The aim of this work was to evaluate the effect of hypoglossal (XIIth) nerve crushing on hypoglossal motoneurone (HMN) discharge in response to the basal inspiratory afferent drive and its chemosensory modulation by $CO_2$. The evolution of the lesion was assessed by recording the compound muscle action potential evoked by XIIth nerve stimulation, which was lost on crushing and then recovered gradually to control values from the second to fourth weeks post-lesion. Basal inspiratory activities recorded 7 days post-injury in the nerve proximal to the lesion site, and in the nucleus, were reduced by 51.6% and 35.8%, respectively. Single unit antidromic latencies were lengthened by lesion, and unusually high stimulation intensities were frequently required to elicit antidromic spikes. Likewise, inspiratory modulation of unitary discharge under conditions in which chemoreceptor drive was varied by altering end-tidal $CO_2$ was reduced by more than 60%. Although the general recruitment scheme was preserved after XIIth nerve lesion, we noticed an increased proportion of low-threshold units and a reduced recruitment gain across the physiological range. Immunohistochemical staining of synaptophysin in the hypoglossal nuclei revealed significant reductions of this synaptic marker after nerve injury. Morphological and functional alterations recovered with muscle re-innervation. Thus, we report here that nerve lesion induced changes in the basal activity and discharge modulation of HMNs, concurrent with the loss of afferent inputs. Nevertheless, we suggest that an increase in membrane excitability, reported by others, and in the proportion of low-threshold units, could serve to preserve minimal electrical activity, prevent degeneration and favour axonal regeneration.**

(Received 18 December 2003; accepted after revision 13 April 2004; first published online 16 April 2004)
**Corresponding author** B. Moreno-López: Área de Fisiología, Facultad de Medicina, Plaza Falla, 9, 11003 Cádiz, Spain. Email: bernardo.moreno@uca.es

Trophic interactions between motoneurones and their target myocytes are necessary for maintaining the functional specializations of both cells types (Kuno *et al.* 1974; Foehring *et al.* 1987*a*,*b*). Consequently, when functional connectivity is disrupted, profound alterations in structural and physiological properties of both motoneurone and muscle are observed. Axotomy induces changes in axonal, synaptic and intrinsic membrane properties that are similar in spinal (Eccles *et al.* 1958; Kuno & Llinás, 1970*a*,*b*; Heyer & Llinás, 1977; Gustaffson, 1979; Brännström & Kellerth, 1998) and hypoglossal motoneurones (HMNs; Sumner, 1975; Takata *et al.* 1980; Takata & Nagahama, 1984). Axotomy-induced alterations include chromatolysis, retraction of dendritic arborization, enhanced somato-dendritic excitability, decreased axonal conduction velocity and massive loss of afferent synaptic inputs (reviewed in Mendell, 1984; Titmus & Faber, 1990; González-Forero *et al.* 2004). These alterations are usually transient and the normal electrical and synaptic properties of motoneurones recover with muscle re-innervation, even when the re-innervation is crossed or occurs with non-natural targets (Foehring *et al.* 1986, 1987*a*,*b*)

Although much of this previous work has been directed towards defining the response of motoneurones to muscle disconnection, emphasis has usually been placed on

© The Physiological Society 2004 DOI: 10.1113/jphysiol.2003.059972

the electrical and synaptic effects in synaptically silent preparations. Little is known about the discharge activity and rate modulation of axotomized motoneurones under normal afferent synaptic drive. Related work on this issue has been reported for axotomized abducens motoneurones recorded in chronic cat preparations (Delgado-García *et al.* 1988). However, as noticed by these authors, excitability is reduced in axotomized abducens motoneurones, and so their results differ from those described in axotomized spinal and HMNs in which excitability is increased. Likewise, in such studies contralateral eye position was taken as a reference index for the control afferent synaptic drive, despite the possibility that compensatory motor adaptations in the non-treated side can occur (Moreno-López *et al.* 1997). Knowledge of the discharge activity and modulation of axotomized motoneurones in response to physiological patterns of afferent activation has a crucial importance since (a) axotomy-induced increases in membrane excitability and decreases in synaptic efficacy would be expected to have an opposite influence on firing activity, and (b) it would determine the levels of electrical activity in regenerating axotomized motoneurones, which in turn have been shown to affect both the speed and the precision for target re-innervation (Al-Majed *et al.* 2000; Brushart *et al.* 2002).

The tongue participates in diverse essential motor tasks including respiration-related movements; this function is very important for keeping open upper airways during breathing. These breathing-related movements rely on the coordinated actions of protruder (genioglossus) and retractor (hypoglossus and styloglossus) muscles (Sawczuk & Mosier, 2001). In the hypoglossal nucleus (HN), most motoneurones discharge bursts of action potentials synchronized with respiratory phases, even though the great majority of hypoglossal respiratory activity is inspiratory (Hwang *et al.* 1983*a*). During inspiration, HMNs are synaptically excited by pre-motor neurones located within the medulla and pons (Ono *et al.* 1994; Peever *et al.* 2002). A great advantage for our purpose is that, while most oro-facial motor drive is suppressed following decerebration, respiratory afferent activity on HMNs persists (Wang & Nims, 1948; Hwang *et al.* 1983*a*,*b*). Additionally, in *in vivo* decerebrated, and lightly anaesthetized preparations, respiratory activity can be modulated by changes in arterial blood $CO_2$ and $O_2$ pressures (Cohen, 1968; Hwang *et al.* 1983*a*,*b*).

In this work we report that (1) axonal injury induces a depression in firing activity of HMNs, (2) motoneurone sensitivity to afferent drive modulated by changes in end-tidal $CO_2$ was also reduced following XIIth nerve crushing, (3) synaptophysin immunoreactivity was reduced after lesion, and (4) the morphofunctional alterations were reversible, and recovered in parallel with the compound muscle action potential. We conclude that previously reported increases in motoneurone excitability do not completely compensate for the effects of axotomy-induced deafferentation, which accounts for the observation that the inspiratory discharge of HMNs is reduced both under basal conditions and conditions of altered chemoreceptor drive. Possible implications in the speed and selectivity of regenerative processes following peripheral nerve injury are discussed.

## Methods

### Subjects

Adult male Wistar rats weighing 250–400 g, obtained from an authorized supplier (Animal Supply Services, University of Cádiz, Spain), were used in this study. Animals were individually housed in cages with water and food pellets available *ad libitum*, under temperature-controlled conditions at $21 \pm 1^{\circ}$C, with a cycle of 12 h light and 12 h darkness. Experiments were performed in accordance with the European Union directive 609/86/CEE and with Spanish legislation (RD 233/89) on the use and care of laboratory animals, and approved by the local Animal Care and Ethics Committee. All surgical procedures were carried out under aseptic conditions.

### XIIth nerve injury

Animals were anaesthetized with chloral hydrate ($0.5\ g\ kg^{-1}$; I.P.). A sufficient depth of anaesthesia was judged from the absence of withdrawal reflexes. The right XIIth nerve was isolated from surrounding tissue and the common nerve trunk was then thoroughly crushed with microdissecting tweezers, applied for 30 s. The lesion was made just proximal to the bifurcation into lateral and medial branches (Fig. 1). The incision was sutured, cleaned with an aseptic solution (povidone–iodine) and the animals were allowed to survive 1, 3, 7, 15, 22, 30 or 45 days after the crushing. In the control group this surgery was absent, and in sham-operated animals the nerve was dissected but crushing was omitted. All animals received one post-operative injection of penicillin ($20\,000$ i.u. $kg^{-1}$; I.M.) in order to prevent infection. Pirazolone ($0.1\ mg\ kg^{-1}$; I.M.) was given on awakening for post-operative analgesia. At least three animals per experimental condition were used.

© The Physiological Society 2004

### Electromyographic and electroneurographic recordings

To study the time course effects of nerve injury on compound muscle action potential (CMAP) and basal activity of the XIIth nerve, experimental animals were anaesthetized as indicated above, both XIIth nerves were dissected and Teflon-isolated silver bipolar electrodes were placed 3–4 mm proximal to their bifurcation (Fig. 1). Electrodes were electrically isolated from neighbouring tissue with Vaseline jelly and parafilm. CMAP was recorded by means of two stainless steel Teflon-coated hook electrodes implanted in the genioglossus muscle. The XIIth nerve was stimulated and the orthodromic field potential elicited in the muscle (Fig. 1*A*) was recorded, amplified, and low-pass filtered to 3 kHz. Stimuli were single cathodic square pulses of 50 $\mu$s at 1 Hz and the current intensity applied was three times the threshold current for CMAP detection. In all animals tested at 1, 3 and 7 days, threshold could not be determined, in which case stimulation intensities fivefold higher than threshold measured on the control side ($< 0.1$ mA) were tested.

Electroneurographic activity was recorded using the same electrodes implanted in the XIIth nerves for stimulation purposes (Fig. 1*B*, upper trace). Spontaneous activity from both nerves in anaesthetized animals was recorded in monopolar mode, AC-coupled, amplified and filtered (10 Hz to 10 kHz). The signals were visualized, transferred and stored in a computer. Animals used in these experiments were finally perfused, as indicated below, and the brainstems removed and stored for later histological processing.

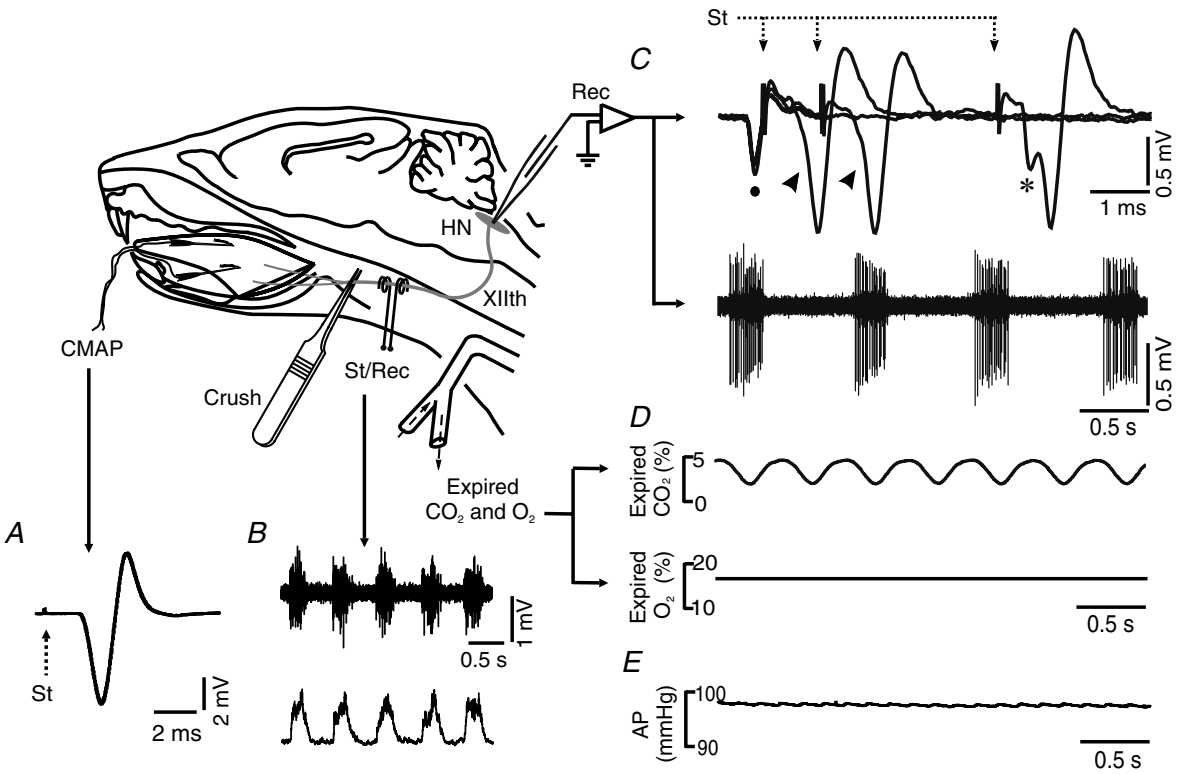


**Figure 1. Schematic diagram of the experimental preparations**
In the first experimental approach, the compound muscle action potential (CMAP; *A*) and the XIIth nerve activity (*B*, upper trace) were recorded in anaesthetized animals by means of electrodes implanted in the genioglossus muscle and in the XIIth nerve (St/Rec), respectively. Analysis of burst activity in neurograms was performed on the integrated XIIth nerve signal (*B*, lower trace). In the second experimental approach, unitary discharge activity of hypoglossal motoneurones (HMNs; *C*, lower trace), expired $CO_2$ and $O_2$ (*D*) and arterial pressure (AP; *E*) were obtained in decerebrated, vagotomized rats, which had been injected with a neuromuscular blocking agent and lightly anaesthetized. Hypoglossal motoneurones were identified by their antidromic activation from the electrode (St/Rec) implanted in the XIIth nerve and by the collision test (*C*, upper trace) between spontaneous orthodromic (●) and evoked antidromic action potentials (*). Shortening the interval between these resulted in antidromic spike occlusion (arrowheads). Arrows in *A* and *C* indicate stimulus artifact. HN, hypoglossal nucleus.

© The Physiological Society 2004

### Extracellular recordings of HMNs

Rats were anaesthetized as previously indicated. Atropine sulphate (0.05 mg) and dexamethasone sodium phosphate (0.2 mg) dissolved in saline were administered intramuscularly to minimize airway fluid secretion and brain oedema, respectively. A ventral approach was used to cannulate trachea, bladder, and femoral artery and vein. Bipolar stimulating electrodes were bilaterally implanted on XIIth nerves (Fig. 1). Vagotomy was bilaterally performed to eliminate the effect of pulmonary afferent signals on central respiratory drive. Then each animal was placed in a stereotaxic frame, injected with the neuromuscular blocking agent gallamine triethiodide (20 mg $kg^{-1}$ I.V. initially and supplemented with 4 mg $kg^{-1}$ as needed) and mechanically ventilated. Expired $CO_2$ and $O_2$ were continuously monitored (Eliza duo, Gambro Engström, Bromma, Sweden), and data were stored in a computer. The end-tidal $CO_2$ ($ET_{CO_2}$) was changed (3–3.5 to 7–7.5%) as required by adjusting ventilation parameters (tidal volume and/or respiratory rate). In all experiments, expired $O_2$ was always between 19% and 14%, and so was higher than those values below which hypoxia-induced alterations have been reported (Hwang *et al.* 1983*a*). Femoral arterial blood pressure was monitored and maintained between 80 and 110 mmHg (Fig. 1*E*). The heart rate was similar in all experimental conditions (370–445 beats $min^{-1}$) as measured from the pulse pressure wave. When necessary, a modified Ringer solution (2 ml 1 M $NaHCO_3$ and 10 ml 5% glucose in 38 ml Ringer solution) was infused through the femoral vein. Rectal temperature was monitored and maintained at $37 \pm 1^{\circ}$C by placing the animal on a temperature-controlled heating pad. Precollicular decerebration, confirmed by post-mortem examination, was performed after craniotomy. Some anaesthetics, including chloral hydrate, can affect respiratory parameters (Hwang *et al.* 1983*b*). Therefore, discontinuation of anaesthesia could progressively modify respiratory function. For this reason, although decerebration rendered the animals insentient, low supplemental doses of chloral hydrate (0.05 g $kg^{-1}$ $h^{-1}$) were given. This procedure allowed the basal burst rate (BR) to be kept steady during the recording session. Before the beginning of neuronal recording, animals were allowed to stabilize for 30 min after decerebration, maintaining $ET_{CO_2}$ at 4.8–5.2%.

Extracellular recordings were carried out with glass micropipettes bevelled to a resistance of 1–3 MΩ and filled with a conductive solution of 2 M NaCl. Micropipettes were advanced with a three-axis micromanipulator and visually guided to reach the brainstem at the level of the obex. Then the micromanipulator was laterally displaced 0.2–0.5 mm and advanced through the brainstem down to the HN. The characteristic inspiratory pattern of the HN was heard in the audio monitor and its localization was confirmed by the presence of the antidromic field potential produced by electrical stimulation of the ipsilateral XIIth nerve (Fig. 1*C*). The stimuli consisted of cathodic square pulses (50 $\mu$s, < 0.1 mA, 1 Hz). HMNs were positively identified by their antidromic activation from the XIIth nerve and by the collision test between the orthodromic and antidromic action potentials (Fig. 1*C*, upper trace). The extracellular neuronal activity was recorded with the aid of a high-impedance circuit located in a head-stage close to the preparation. The electrical signals were amplified and filtered at a bandwidth of 10 Hz to 10 kHz for display and digitization purposes. Responses of HMNs were recorded initially at normocapnia ($ET_{CO_2}$ = 4.8–5.2%), and then in response to a change in $ET_{CO_2}$ from hypocapnic (∼3%) to hypercapnic (∼7.5%) conditions. From basal conditions, motoneurones were recorded during a slow increase in $ET_{CO_2}$ up to 7–7.5% followed by a slow decrease down to 3–3.5% and finally recovery to 4.8–5.2%. For each analysed motoneurone, the test was completed in ∼5 min. Motoneurones remained well isolated during the entire test. Only motoneurones discharging at basal conditions were considered in this study. During extracellular recordings, bursts of enhanced activity of the HN were clearly discriminated on the background noise (Fig. 6*A* and *B*). Since HN activity has been shown to be mostly inspiratory (Hwang *et al.* 1983*a*,*b*), bursts were used as indicative of the inspiratory phase. Then, we classified HMNs as inspiratory, expiratory or non-respiratory tonic units according to their relationship with the inspiratory burst activity of the HN. Only inspiratory HMNs were used in this study.

### Data storage and analysis

**General.** Electromyographic, electroneurographic and unitary discharge signals, percentages of expired $CO_2$ and $O_2$, and arterial pressure recordings were amplified, filtered, transferred and stored in a computer through a PowerLab/8SP A/D interface (ADInstruments, Castle Hill, Australia). Data acquisition was performed using the Scope and Chart software for CMAP (100 kHz sampling rate) and the remaining signals (40 kHz sampling rate), respectively. The same software was used for off-line analysis of data. Values are always expressed as mean ± S.E.M.

© The Physiological Society 2004

**Electromyogram and electroneurogram.** To assess muscle de-innervation and study the time course of re-innervation, CMAPs evoked by XIIth nerve stimulation were analysed at different times after crushing. Peak latency and amplitude of CMAP were measured with respect to the stimulation artifact and baseline, respectively, in control and experimental animals. The electroneurographic signals were integrated (Fig. 1*B*, lower trace; $\tau = 20$ ms) and measures were taken using a parabola automatically fitted to the integrated burst activity provided by the software (insets in Fig. 4*B–D*). Several burst parameters including area, duration (BW; burst width) and 10–90% slope ($\text{slope}_{10-90}$) from the baseline were obtained by this method (Fig. 4*B–D*). Data were averaged from 10 CMAPs and 30 bursts for electromyographic and electroneurographic recordings, respectively, and expressed relative to the contralateral control side. Comparison between experimental and control values, at different post-injury times, was performed using the non-parametric Mann-Whitney *U* test.

**Neuronal activity.** Unitary HMN activity was recorded and stored together with arterial femoral pressure and expired $CO_2$ and $O_2$ percentages in the same file (Figs 1*C–E* and 2). The histogram of instantaneous firing rate (FR, i.e. the reciprocal of the interval between two adjacent spikes) and the $ET_{CO_2}$ were calculated and displayed from the original recordings (Fig. 2). Bursts were automatically selected using a macro and several parameters were saved in a data pad for subsequent statistical analysis. The following parameters were measured in each motoneurone (Fig. 2): mean FR (mFR, in spikes $s^{-1}$) averaged over the duration of the inspiratory burst, peak FR (pFR, in spikes $s^{-1}$), duration (DB, in ms) and number of spikes (SB, in spikes), all of these relative to burst events, and the cycle duration was used to calculate burst rate (BR; in bursts $min^{-1}$). Data were processed for statistical analysis with PC-based statistical software. Several parameters were correlated with the variable $ET_{CO_2}$ (as a percentage) using linear regression analysis. Data plots were fitted by linear functions with the equation: $y = mx + n$; where $y$ is mFR, pFR, SB, DB or BR; $x$ is $ET_{CO_2}$; $n$ is the intercept ($I$), i.e. the theoretical value when $ET_{CO_2} = 0\%$; and $m$ is the slope, i.e. the neuronal gain or sensitivity ($S$) for each parameter with respect to $ET_{CO_2}$ variation. Five equations characterizing the behaviour of a HMN in response to changes of $ET_{CO_2}$ could be obtained: (a) $\text{mFR} = S_{\text{mFR}}ET_{CO_2} + I_{\text{mFR}}$; (b) $\text{pFR} = S_{\text{pFR}}ET_{CO_2} + I_{\text{pFR}}$; (c) $\text{SB} = S_{\text{SB}}ET_{CO_2} + I_{\text{SB}}$; (d) $\text{DB} = S_{\text{DB}}ET_{CO_2} + I_{\text{DB}}$ and (e) $\text{BR} = S_{\text{BR}}ET_{CO_2} + I_{\text{BR}}$. The units for slopes in these equations were: spikes $s^{-1}$ $\%^{-1}$ for $S_{\text{mFR}}$ and $S_{\text{pFR}}$, spikes $\%^{-1}$ for $S_{\text{SB}}$, ms $\%^{-1}$ for $S_{\text{DB}}$ and bursts $min^{-1}$ $\%^{-1}$ for $S_{\text{BR}}$. Data were grouped and averaged in intervals of 0.2% of $ET_{CO_2}$. More than 4 bursts were included in each interval and at least 15 intervals were used for each linear regression analysis. Only regressions with $r \geq 0.8$ and $P < 0.001$ were considered for statistical analysis. One-way ANOVA and *post hoc* comparison tests at a level of significance of $P < 0.05$ were used for the

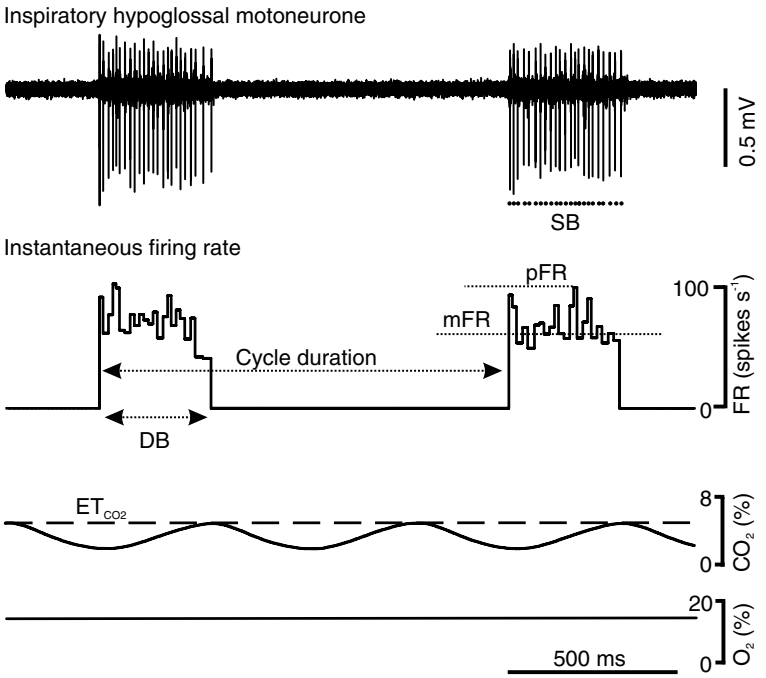


**Figure 2. Characterization of firing properties of the hypoglossal motoneurones**
From top to bottom, traces represent the extracellularly recorded spike discharge for a control inspiratory hypoglossal motoneurone, the instantaneous firing rate (FR, in spikes $s^{-1}$; bin width = 25 $\mu$s) and the partial pressures of $CO_2$ and $O_2$ as a percentage of the expired air, respectively. End-tidal $CO_2$ ($ET_{CO_2}$) is indicated on the $CO_2$ record as a dashed line. Mean (mFR) and peak (pFR) firing rates, and number of spikes (SB) in each burst, as well as burst (DB) and cycle durations, were measured. Burst and cycle parameters were analysed in relation to simultaneous $ET_{CO_2}$ measurements.

© The Physiological Society 2004

comparison of the mean parameters relative to different experimental conditions.

### Synaptophysin immunohistochemistry

Animals used for electroneurographic and electromyographic recordings received a supplemental dose of chloral hydrate (0.1 g kg$^{-1}$; I.P.), and were transcardially perfused first with phosphate-buffered saline (PBS), followed by 4% paraformaldehyde in 0.1 M phosphate buffer (PB), pH 7.4, at 4°C. The brains were removed, post-fixed for 2 h in the same fixative solution, and cryoprotected by overnight immersion in 30% sucrose in PB at 4°C. Coronal sections from the brainstem, 40 $\mu$m thick, were obtained using a freezing microtome. Brainstem sections containing the HNs were first incubated in a solution containing 2% (v/v) hydrogen peroxide and 60% (v/v) methanol in PBS, to block endogenous peroxidase activity. Then the tissue was rinsed in PBS and immersed in 2.5% (w/v) bovine serum albumin, 0.25% (w/v) sodium azide and 0.1% (v/v) Triton X-100 in PBS for 30 min, followed by overnight incubation at room temperature with specific anti-synaptophysin rabbit polyclonal antibody (1 : 100; Zymed Laboratories, San Francisco, CA, USA). Subsequently, the tissue was rinsed with PBS and incubated for 1 h at room temperature with a biotinylated anti-rabbit IgG (1 : 800; Sigma) as secondary antibody. Biotin was detected by means of the avidin–biotin–peroxidase system (Pierce, Rockford, IL, USA) using 3,3′-diaminobenzidine tetrahydrochloride as chromogen. Sections were mounted on slides, dehydrated, covered with DePeX and visualized under light microscopy. Omission of primary antibody resulted in no detectable staining (Fig. 9*G*).

Synaptophysin immunoreactivity was analysed using a BX60 microscope (Olympus). Images corresponding to single optical sections throughout the HN were obtained with a digital camera (DP10, Olympus). Right (experimental) and left (control) sides were captured (×100) in the same image, with identical setting parameters. Images were processed for background subtraction to obtain the maximum dynamic range of intensities (from 0 to 100) and analysed using the Microimage software (Olympus). In all cases, the area delimiting the HN was manually traced and for each image, the density histogram and mean optical density (i.e. the average of pixel intensity in the outlined area) of synaptophysin immunolabelling was obtained in both the control and experimental hypoglossal regions. Data were collected from 4–6 sections per animal. Three animals were used per experimental condition. The percentage decrease between experimental and control sides was compared at different post-lesion times using the non-parametric Mann-Whitney *U* test.

## Results

### Neuromuscular function integrity

In anaesthetized animals, orthodromic CMAPs evoked by single-pulse stimulation of XIIth nerve were recorded to evaluate the functionality of neuromuscular junctions. The amplitude and latency of the resulting wave were taken as an index of lesion and recovery degree of the motor nerve. In controls, CMAP was biphasic, with a large negative wave followed by a small positive wave (Fig. 3*A*). The negative wave had $2.5 \pm 0.04$ ms of latency and $9.5 \pm 2.0$ mV of amplitude. The recorded potential was postsynaptic, since it was eliminated in acute experiments by the blockade of acetylcholine receptors with a neuromuscular blocking agent (gallamine triethiodide; 3 mg kg$^{-1}$, I.M.) injected in the genioglossus muscle. In all experiments performed 1, 3 or 7 days after crushing, CMAP was completely eliminated, even when supramaximal ($< 0.1$ mA) nerve stimulation was applied. No signs of recovery were observed during the first week (Fig. 3*B* and *E*). These results indicated that our method of nerve crush effectively disconnected most HMNs from their targets.

The first evidence of muscle re-innervation was obtained at 15 days after crushing, with CMAPs of significantly lower amplitude ($0.4 \pm 0.03$ mV) and longer latency ($4.7 \pm 0.6$ ms) than in the control side (Fig. 3*E* and *F*). Moreover, CMAPs recorded at 15 and 22 days post-lesion usually showed a polyphasic profile, with a variable number of negative peaks, which could be interpreted as resulting from the asynchronous arrival of pre-synaptic motor impulses. Subsequently, there was a slow and progressive recovery of CMAP towards control values (Fig. 3*C*–*F*). Recovery of CMAP amplitude ($6.9 \pm 1.8$ mV) was noticed at 30 days after crushing, although a slight difference in latency ($3.1 \pm 0.2$ ms) was still evident (Fig. 3*D*–*F*). Therefore, after an initial phase of reduced and asynchronous muscle activation, during re-innervation most CMAP parameters progressively recovered in parallel with the narrowing of the range of axonal conduction velocities. Since hypoglossal nerve regeneration lasted 30 days, we examined nerve activity, and unitary discharge properties and synaptic density in the HN, at selected time points before (1, 3 and/or 7 days) and during target re-innervation (15, 22 and/or 30 days).

© The Physiological Society 2004

### Depression of XIIth nerve activity after crushing

We investigated possible alterations in HMN pool activity by means of nerve recordings carried out proximal to the lesion at 1, 3, 7, 15, 22, 30 and 45 days after nerve crushing in the same animals as those used for electromyographic studies. Activity was expressed as the ratio between crushed and intact sides and compared with data from control animals. Recordings were integrated and area, BW and slope$_{10–90}$ were measured to characterize nerve burst activity. In control animals, electrical activity of both XIIth nerves was characterized by a rhythmic inspiratory discharge (Fig. 4*A*). After nerve injury, the inspiratory-related activity was reduced in a time-dependent manner (Fig. 4*A–C*). Significant reductions in nerve activity appeared as soon as 1 day post-lesion and declined thereafter, reaching a minimum at 15 days post-crushing (Fig. 4*B*). The integrated area of XIIth nerve bursts was reduced by $23.8 \pm 7.6\%$, $41.1 \pm 14.6\%$ and $51.6 \pm 8.8\%$ at 1, 3 and 7 days post-injury, respectively. Maximum significant depression occurred 15 days after crushing (62.2%) and a rapid increase towards control values was noticed 7 days later ($93.6 \pm 8.9\%$ of control; Fig. 4). Integrated activity was maintained at control levels when measured on subsequent days (Fig. 4*B*).

Besides integrated burst area, other burst parameters were also modified after crushing. This is the case for the slope$_{10–90}$ of burst, a parameter that was reduced by $49.0 \pm 4.9\%$ at 7 days, and whose time course of recovery was parallel to that indicated for mean integrated area (Fig. 4*C*). Mean values of BW were not significantly affected by nerve crushing at any time post-injury (Fig. 4*D*). In the sham-operated group, differences with respect to control were not observed (Fig. 4). Therefore, reduced basal XIIth nerve activity was transitory and persisted as long as the CMAP was absent, suggesting that motor nerve and muscle were disconnected. Early after re-innervation was initiated at the second week, a fast and complete re-establishment of normal nerve activity occurred (Figs 3 and 4). Three rats per experimental condition were used in this study, since electroneurographic changes were very homogeneous; results from these experiments were mainly used to select the time points for unitary extracellular HMN recordings.

### Slowing of conduction velocity in proximal motor axons

The HN was located by means of the antidromic field potential produced by the electrical stimulation of the ipsilateral XIIth cranial nerve (Figs 1*C* and 5*A*, arrowheads). The antidromic spike of HMNs appeared summated on the antidromic field, and in some cases it was somewhat difficult to distinguish the neuronal spike from the antidromic field. To ascertain that the recorded neurone was the same as that activated antidromically, the collision test was used. An orthodromic spike was fed through the window discriminator and the generated pulse was used to trigger, at a certain latency, the antidromic stimulus (Fig. 1*C*). By shortening the interval between

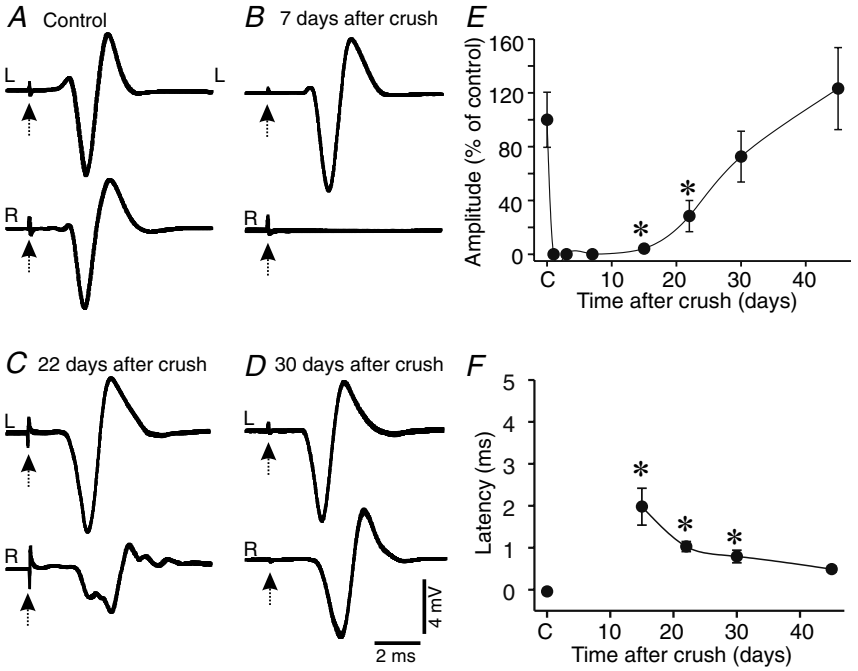


**Figure 3. Time course of muscle re-innervation following XIIth nerve crushing**
*A–D*, compound muscle action potentials (CMAPs) evoked by single shock stimulation (arrow) of XIIth nerve in control condition and at indicated post-lesion times. For comparison, muscle responses following left (L, control side) and right (R, experimental side) XIIth nerve stimulation are illustrated. *E* and *F*, time course of changes and recovery in the mean CMAP amplitude (*E*, expressed as percentage of control) and latency (*F*, expressed as difference from control side) following XIIth nerve lesion. Values are means ± S.E.M. for 3 animals. *Statistically significant differences ($P < 0.05$; non-parametric Mann-Whitney *U* test) with respect to the control (C, unoperated) group.

© The Physiological Society 2004

the spontaneous spike and the antidromic stimulus it was possible to occlude the antidromic spike, revealing only the antidromic field potential and demonstrating unequivocally that the recorded neurone was a HMN (Figs 1 and 5*A*). Only HMNs meeting this criterion and showing inspiratory-related activity were included in this study. The antidromic latency of control HMNs followed a bell-shaped distribution ($P < 0.01$, *F*-Snedecor test) of mean $1.1 \pm 0.02$ ms (Fig. 5*B* and *C*).

Nerve crushing induced a slight increase in antidromic latencies that was apparent 3 days after injury (earliest time point measured), although their mean value

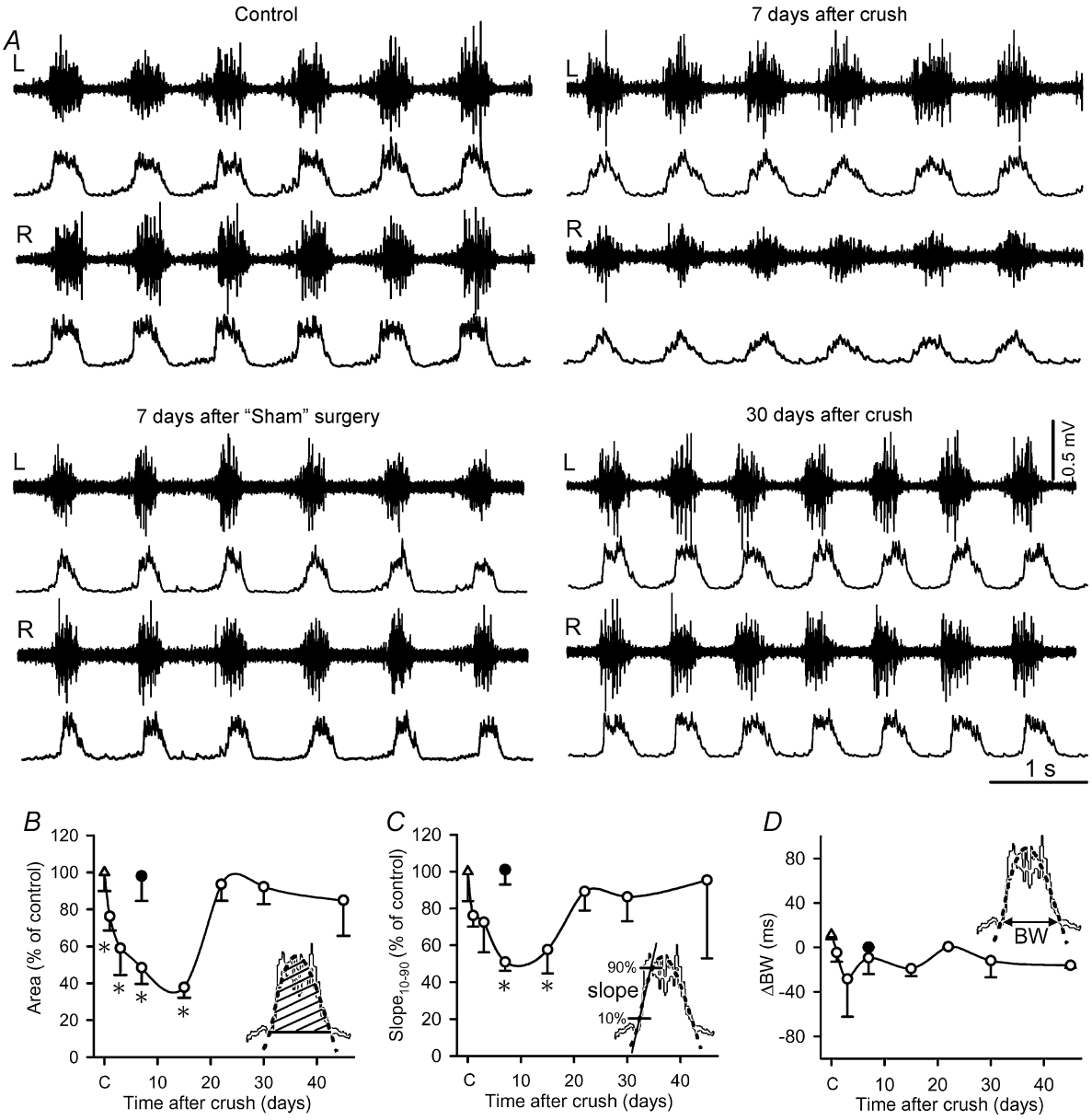


**Figure 4. Time course of changes in nerve activity following XIIth nerve crushing**
*A*, bilateral recordings from XIIth nerves and their integrated signal in control condition, and at indicated post-lesion times. R and L indicate right (experimental) and left (control) sides, respectively. *B–D*, time course of changes in the mean values for the burst area (*B*), 10–90% slope ($Slope_{10–90}$; *C*) and duration (BW; *D*), measured on the integrated hypoglossal nerve discharge, after XIIth nerve crushing (○), relative to control (C, △) and sham (●) groups. Insets: grey traces, integrated burst activity; dotted traces, automatically adjusted parabola (see details in Methods). In *D*, differences (in ms) between crushed and control sides are indicated in the ordinate. Values represent means ± S.E.M. for 3 animals. *Statistically significant differences ($P < 0.05$; Mann-Whitney *U* test) with respect to the control (unoperated) group.

© The Physiological Society 2004

(1.2 ± 0.04 ms) did not significantly differ from control. However, significant differences were reached at successive post-injury times, with increases to 1.4 ± 0.04 ms and 1.6 ± 0.06 ms at 7 and 15 days, respectively (Fig. 5). Distribution histograms showed that, besides a general displacement to the right, the appearance of cells with abnormally long latencies was particularly noticeable (Fig. 5*B*). Whereas latencies longer than 2 ms were absent in the control group, the proportion of motoneurones with such a feature was 5.5% and 19.0% of total pools sampled at 7 and 15 days, respectively. The averaged latency of motoneurones recorded in the sham group at 7 days (1.1 ± 0.05 ms) was not different from control values. Moreover, it was usually observed that spike generation in crushed motoneurones included in these groups needed higher stimulation intensities. These results indicate that nerve crushing leads to changes in the properties of proximal motor axons, which reduced their conduction velocities and excitability. Mean latency reached control values at 30 days post-lesion (1.2 ± 0.03 ms), by which time CMAP and neurogram parameters were fully recovered.

### Basal activity of HMNs

The effects of nerve injury on neurogram activity could be explained by the blockade of impulse conduction along axons and/or diminished activity of the motoneurone pool. To evaluate this issue, unitary basal firing activities of HMNs in basal conditions ($ET_{CO_2}$ = 4.8–5.2%) were

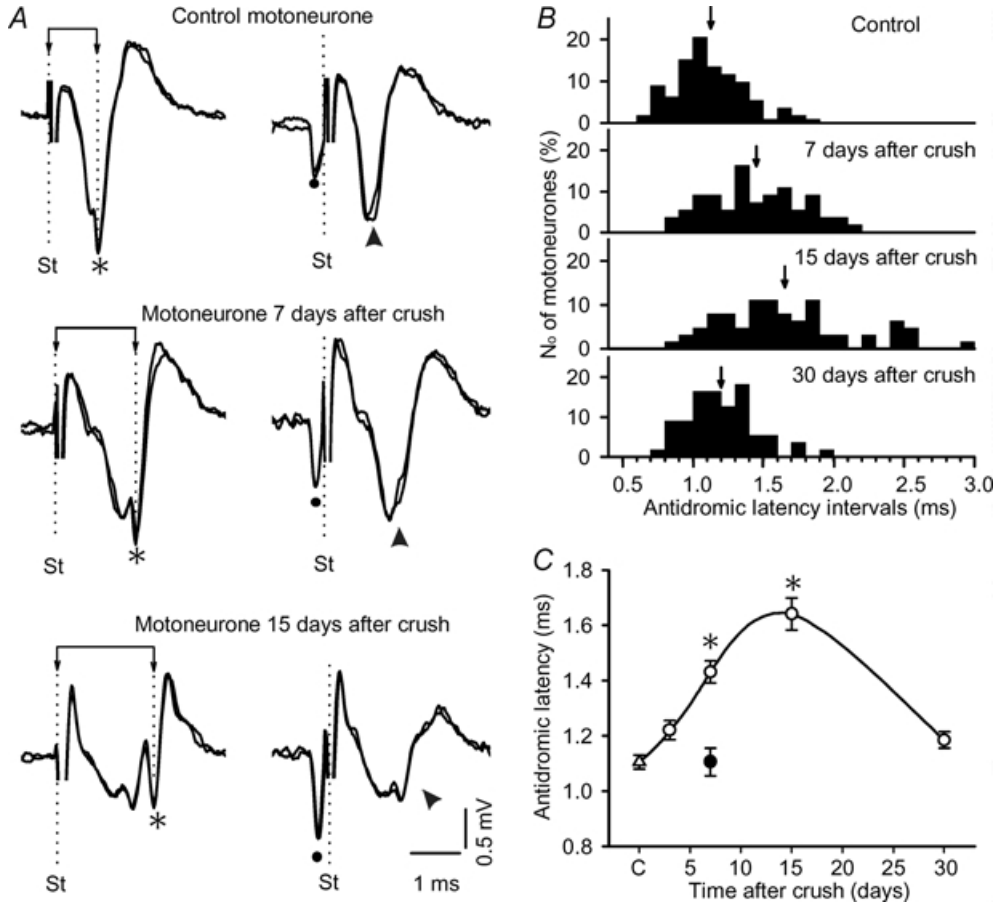


**Figure 5. Axonal conduction alterations after XIIth nerve crushing**
*A*, representative antidromic activations (*) and collisions (arrowhead) in motoneurones recorded in control, and at number of days indicated after XIIth nerve crushing. Note that activation latency, measured as the time difference between XIIth nerve stimulation (St) and the negative peak of the antidromic spike (*), was longer in motoneurones recorded after nerve lesion. *B*, histograms showing the distribution and mean values (↓) of the antidromic activation latencies obtained in the control ($n$ = 112), and at 7 ($n$ = 55), 15 ($n$ = 65) and 30 ($n$ = 55) days post-lesion. *C*, time course of changes in the antidromic activation latency (means ± S.E.M.) after XIIth nerve crushing (○), relative to the control (C, Δ) and sham (●) groups. *Significant differences ($P$ < 0.05; one-way ANOVA; *post hoc* Dunnett's method) relative to control group.

© The Physiological Society 2004

recorded in decerebrated and vagotomized animals under neuromuscular blockade. Burst parameters were measured and averaged using a minimum of 30 bursts per motoneurone to characterize the basal activity of the nucleus at different time points after lesion. Control inspiratory HMNs showed a characteristic respiratory pattern that consisted of bursts of action potentials coincident with the inspiratory phase of breathing, clearly demonstrated by the background nucleus activity (Fig. 6*A*). This pattern was characterized in the control stage by a BR of $43.7 \pm 0.9$ bursts min$^{-1}$ and a mFR of $36.6 \pm 2.5$ spikes s$^{-1}$, with a DB of $361.9 \pm 14.0$ ms (Table 1). All parameters measured are presented in Table 1. At the earliest time point measured, 3 days after crushing, burst parameters underwent a significant reduction that persisted at 7 and 15 days but recovered to

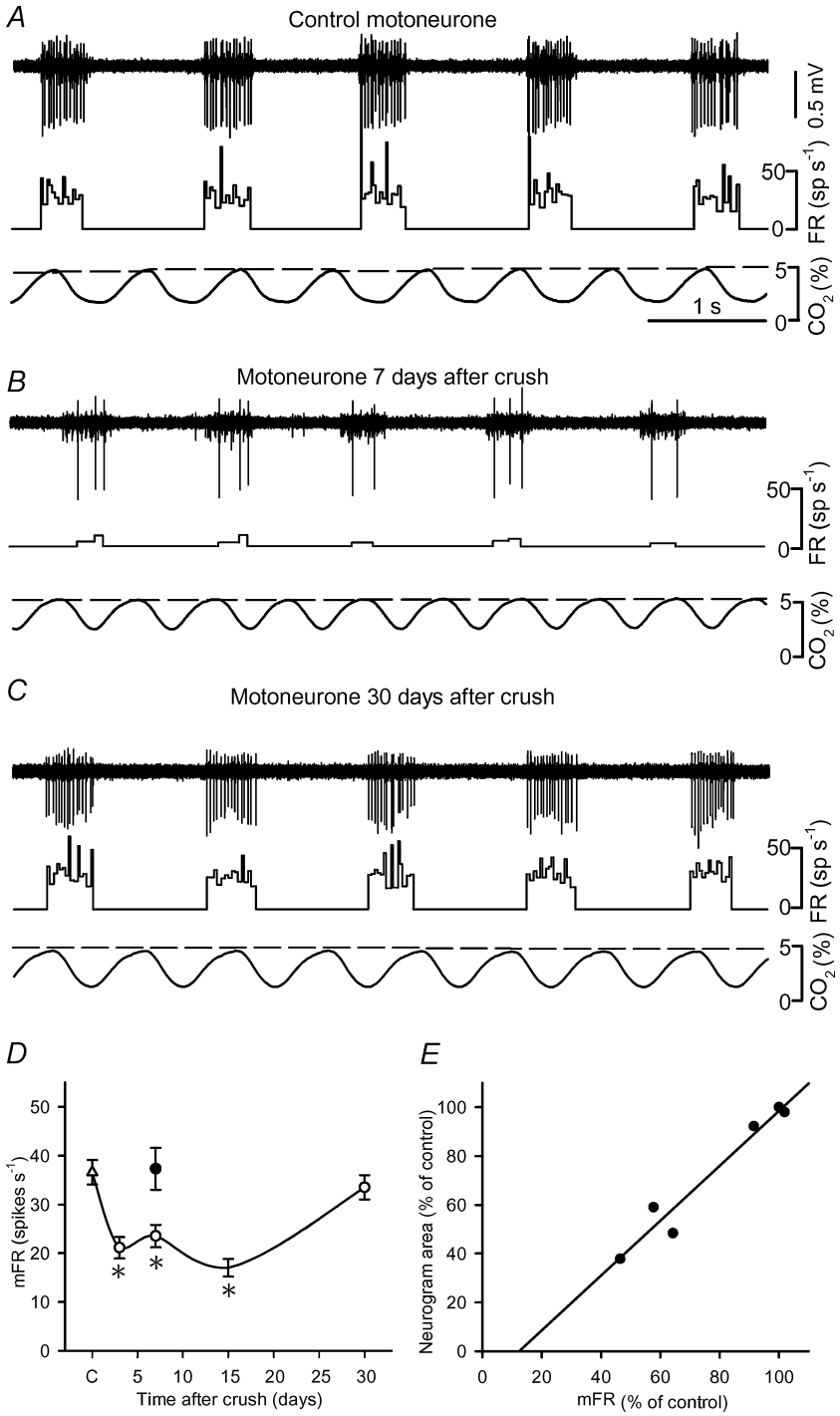


**Figure 6. Basal firing activity of the hypoglossal motoneurones**
*A–C*, representative examples showing the discharge activity of hypoglossal motoneurones recorded at basal conditions ($ET_{CO_2} = 4.8$–$5.2$ %) in the control (*A*), and at 7 (*B*) and 30 days (*C*) following ipsilateral XIIth nerve crushing. For each panel, from top to bottom, traces are the raw signals of extracellularly recorded spike activity, the histogram of instantaneous firing rate (FR, in spikes s$^{-1}$) and the percentage of $CO_2$ (continuous line) and $ET_{CO_2}$ (dashed line) in the expired air. Time scale for all recordings is shown in *A*. *D*, time course of alterations in the mean FR (mFR) per burst, as measured in basal conditions, following XIIth nerve crushing (○), relative to the control (C, Δ) and sham (●) groups. Values represent means ± S.E.M. *Significant differences ($P < 0.05$; one-way ANOVA; *post hoc* Dunnett's method) relative to the control group. *E*, plot of mFR *versus* neurogram area (both expressed as percentage of control) including data points corresponding to the control, sham, and 3, 7, 15 and 30 days post-lesion groups. For each point, the average mFR was calculated from the whole sample of units recorded ($n = 18$–$53$) in decerebrated and vagotomized animals under neuromuscular blockade, and the neurogram area as the mean value for the neurographic recordings ($n = 3$) in anaesthetized animals in the same conditions. This relationship was fitted by the regression line: $y = -14.0 + 1.12x$ ($r = 0.98$; $P < 0.0001$).

© The Physiological Society 2004

**Table 1. Firing properties of inspiratory hypoglossal motoneurones in basal conditions[a]**

| Experimental conditions | *n* | mFR (spikes $s^{-1}$) | pFR (spikes $s^{-1}$) | SB (spikes $burst^{-1}$) | DB (ms) | BR (bursts $min^{-1}$) |
|---|---|---|---|---|---|---|
| Control | 49 | 36.6 ± 2.5 | 100.5 ± 11.1 | 15.1 ± 1.3 | 361.9 ± 14.0 | 43.7 ± 0.9 |
| Sham[b] | 18 | 37.3 ± 4.3 | 105.4 ± 13.7 | 15.3 ± 2.3 | 351.7 ± 26.5 | 37.8 ± 1.6* |
| 3 days post-crushing | 29 | 21.1 ± 2.2* | 49.4 ± 8.4* | 6.9 ± 1.1* | 275.5 ± 25.0* | 36.6 ± 1.0* |
| 7 days post-crushing | 50 | 23.5 ± 2.3* | 57.2 ± 8.1* | 8.7 ± 0.9* | 301.1 ± 13.1* | 44.6 ± 1.0 |
| 15 days post-crushing | 53 | 17.0 ± 1.8* | 41.5 ± 7.4* | 6.4 ± 0.9* | 321.4 ± 23.4* | 43.0 ± 1.3 |
| 30 days post-crushing | 31 | 33.5 ± 2.5 | 101.1 ± 14.1 | 13.5 ± 1.4 | 359.8 ± 21.6 | 45.6 ± 1.4 |

[a]Basal conditions were considered to be when $ET_{CO_2}$ = 4.8–5.2%. [b]Animals were studied at 7 days after sham surgery. *n* represents the number of motoneurones included in the study. Data values are expressed as means ± S.E.M. At least 3 animals were used for each experimental condition. *Significant difference with respect to control group ($P < 0.05$; one-way ANOVA test; *post hoc* Dunnett's method). mFR, mean firing rate; pFR, peak firing rate; SB, number of spikes per burst; DB, duration of burst; BR, burst rate.

**Table 2. Modulatory effects of $ET_{CO_2}$ on discharge properties of inspiratory hypoglossal motoneurones**

| Experimental conditions | [a]$S_{mFR}$ (spikes $s^{-1}$ $\%^{-1}$) | $S_{pFR}$ (spikes $s^{-1}$ $\%^{-1}$) | $S_{SB}$ (spikes $\%^{-1}$) | $S_{DB}$ (ms $\%^{-1}$) | $S_{BR}$ (bursts $min^{-1}$ $\%^{-1}$) |
|---|---|---|---|---|---|
| Control | 8.1 ± 0.7 | 24.7 ± 3.6 | 3.5 ± 0.3 | 17.4 ± 6.6 | 4.6 ± 0.6 |
| Sham[b] | 9.0 ± 0.6 | 28.7 ± 4.5 | 3.7 ± 0.4 | 14.8 ± 7.3 | 4.3 ± 0.7 |
| 3 days post-crushing | 5.4 ± 0.5* | 17.4 ± 2.5 | 2.5 ± 0.4* | 18.0 ± 8.9 | 0.3 ± 0.4* |
| 7 days post-crushing | 2.6 ± 0.8* | 9.8 ± 1.4* | I.0 ± 0.2* | 18.4 ± 6.5 | 4.0 ± 0.6 |
| 15 days post-crushing | 4.0 ± 0.9* | 14.1 ± 1.8* | 2.0 ± 0.2* | 19.8 ± 5.5 | 3.6 ± 0.7 |
| 30 days post-crushing | 8.0 ± 1.6 | 29.8 ± 3.3 | 3.7 ± 0.3 | 25.7 ± 4.5 | 4.2 ± 1.1 |

[a]Sensitivity or gain (*S*) parameters characterizing motoneurone activity were measured in response to $ET_{CO_2}$ changes from 3–3.5% to 7–7.5%. [b]Animals were studied at 7 days after sham surgery. Numbers of motoneurones are as indicated in Table 1. Data values are expressed as means ± S.E.M. At least 3 animals were used per experimental condition. *Significant differences with respect to control group ($P < 0.05$; one-way ANOVA test; *post hoc* Dunnett's method). mFR, mean firing rate; pFR, peak firing rate; SB, number of spikes per burst; DB, duration of burst; BR, burst rate.

control values within 1 month (Fig. 6*B–D*; Table 1). The mFR was reduced by 35.8 ± 6.3% and 53.6 ± 4.9%, relative to control, at 7 and 15 days after crushing, respectively. However, at these times, BRs were similar to control, indicating that although injury induced severe changes in motoneurone basal activity, structures involved in the rhythmogenesis of breathing remained similar to the non-injured condition (Table 1). The BR was slightly decreased 3 days after injury and in the sham condition. This alteration was not associated with changes in other burst parameters in the sham group, indicating that both effects were independent (Table 1; Fig. 6*D*). Different anaesthesia levels could explain BR reduction in these two groups.

To investigate the contribution of basal motoneurone activity reduction to the alterations observed in neurographic recordings, we studied the relationship between the burst area of the integrated neurogram and the mFR of HMNs in the control stage and after nerve injury. Statistical analysis confirmed a linear regression ($r = 0.98$, $P < 0.001$) with a slope of 1.12 and an intercept of –14.0 relating the two parameters (Fig. 6*E*). A slope value close to 1 indicated proportional reductions and parallel recovery in both parameters. The negative ordinate intercept denoted a slightly higher reduction in nerve activity relative to discharge activity in the HN, perhaps explained by the blockade of impulse propagation along proximal axons.

### Discharge activity of HMNs in response to end-tidal $CO_2$ changes

The modulation of discharge activity of inspiratory HMNs was studied in relation to $ET_{CO_2}$ variations; it has been well established that these variations modify respiratory parameters. The discharge pattern of control motoneurones consisted of bursts of action potentials during the inspiratory phase of breathing, and the properties of these bursts were generally modified in response to $ET_{CO_2}$ changes (Fig. 7*A*). The burst activity

© The Physiological Society 2004

of motoneurones was increased when $ET_{CO_2}$ rose and was reduced when $ET_{CO_2}$ decreased (Fig. 7*A*, *C* and *D*). For the $ET_{CO_2}$ range used in our experiments, relationships obtained between mFR, pFR, SB, DB or BR and $ET_{CO_2}$ were linear ($r \geq 0.8$, $P < 0.001$). Data were firstly grouped and averaged in 0.2% intervals of $ET_{CO_2}$ and then plotted and analysed (Fig. 7*C* and *D*). Statistically significant relationships between mFR and $ET_{CO_2}$ were observed in ∼94% of control motoneurones. The slope of the regression line represented the sensitivity or gain of mFR to $ET_{CO_2}$ that in control averaged $8.1 \pm 0.7$ spikes $s^{-1}$ $\%^{-1}$ ($S_{mFR}$ in Fig. 7*D* and *E* and Table 2). Examples of scatter

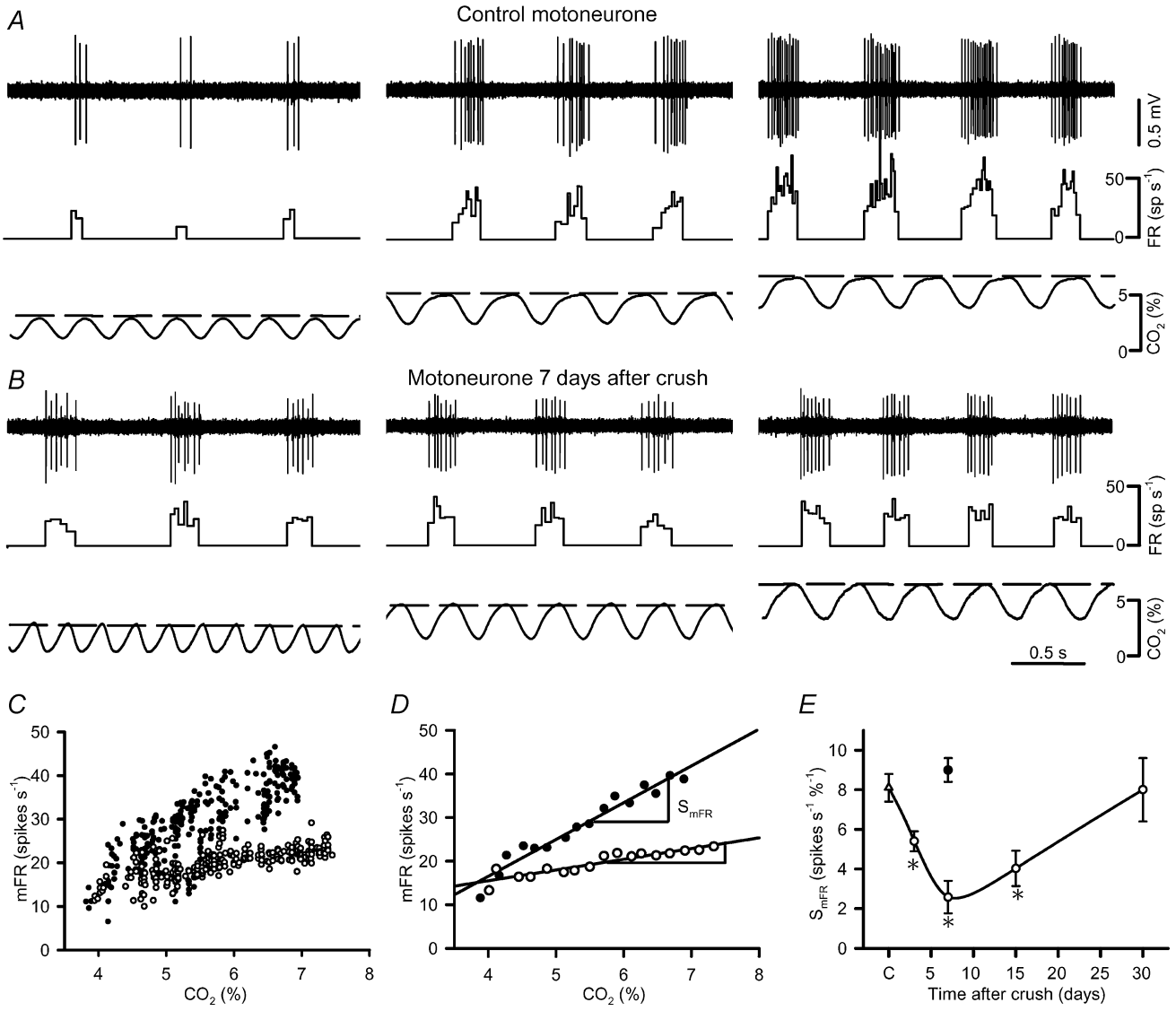


**Figure 7. Effects of XIIth nerve crushing on the $CO_2$-modulated response of hypoglossal motoneurones**
*A* and *B*, discharge activity modulation at different $ET_{CO_2}$ levels for a control motoneurone (*A*) and for a motoneurone recorded 7 days after crushing (*B*). Traces represent the extracellular unitary activity (upper trace), the instantaneous firing rate (FR, in spikes $s^{-1}$; middle trace) and the percentage expired $CO_2$ (continuous line; lower trace) and $ET_{CO_2}$ (dashed line). *C*, plots showing the relationships between mean FR (mFR) per burst and $ET_{CO_2}$ for the motoneurones illustrated in *A* (●) and *B* (○). *D*, same as *C*, but after grouping and averaging data at 0.2% intervals of $ET_{CO_2}$. The slopes of the regression lines represent the neuronal sensitivity or gain to $ET_{CO_2}$ changes ($S_{mFR}$, in spikes $s^{-1}$ $\%^{-1}$). Regression lines are $mFR = -12.27 + 8.44\ ET_{CO_2}$ ($r = 0.97$; $P < 0.0001$) in control and $mFR = 5.68 + 2.45\ ET_{CO_2}$ ($r = 0.92$; $P < 0.0001$) in the experimental motoneurone. *E*, graph representing the time course of changes in $S_{mFR}$ (mean ± S.E.M.) following XIIth nerve crushing (○), relative to the control (C, Δ) and sham (●) groups. *Statistically significant differences ($P < 0.05$; one-way ANOVA; *post hoc* Dunnett's method) relative to control values.

© The Physiological Society 2004

plots obtained for a control motoneurone are shown in Fig. 7*C* and *D* (●). The mean gains of the remaining parameters that were linearly related to $ET_{CO_2}$ are presented in Table 2.

The $S_{mFR}$, $S_{pFR}$ and $S_{SB}$ of HMNs were affected early after lesion. These gains were reduced by $33.3 \pm 6.2\%$, $29.6 \pm 10.1\%$ and $28.6 \pm 11.4\%$ on the 3rd day and reached minimum values on the 7th day with decreases of $68 \pm 9.9\%$, $60.3 \pm 5.7\%$ and $71.4 \pm 5.7\%$, respectively. Although still reduced with respect to the control group, these sensitivities showed initial signs of recovery after the second week when the first signs of muscle re-innervation were observed. One month after the lesion was made, $S_{mFR}$, $S_{pFR}$ and $S_{SB}$ were completely recovered (Fig. 7*E*; Table 2). The discharge pattern of a motoneurone recorded 7 days after lesion is illustrated in Fig. 7*B*, and for comparison the relationship between mFR and $ET_{CO_2}$ was plotted in Fig. 7*C* and *D* (○) together with that obtained for the control motoneurone shown in Fig. 7*A*. No parallel changes were found in $S_{DB}$ and $S_{BR}$ after the lesion (Table 2). The lack of effects on $S_{DB}$ and $S_{BR}$ is crucial for the validation of these results because these parameters are indicative of the integrity of chemosensors and pre-motor structures. Burst parameters were not affected in the sham condition. Thus, nerve lesion decreased the chemoreceptor-modulated responsiveness of HMNs to $ET_{CO_2}$ changes, with no effects on pre-motor respiratory modulation.

### Recruitment of the HMN pool

Threshold distribution and recruitment properties of control and lesioned HMNs were analysed to investigate further if they contributed to determining the functional alterations described above. Theoretical recruitment thresholds were the abscissa intercepts in the mFR–$ET_{CO_2}$ regression lines. For a great proportion of units, recruitment thresholds were negative (48.7% of control motoneurones) and therefore outside the physiological $ET_{CO_2}$ range. The mean threshold in control motoneurones was $-2.2 \pm 0.9\%$ and was not significantly affected at 3 days ($-1.9 \pm 1.8\%$), 7 days ($-5.1 \pm 1.2\%$), 15 days ($-0.1 \pm 0.6\%$) or 30 days ($-0.1 \pm 0.7\%$) after nerve crushing. However, although mean values were not altered by axonal lesion, we noticed changes in threshold distribution and in the relation between this and other functional parameters (Fig. 8).

Recruitment sequence in the control pool appeared graded according to $S_{mFR}$ values, with low-sensitivity units recruited before high-sensitivity cells (Fig. 8*A* and *C*; ●). The relationship between the two parameters was fitted by an exponential curve ($r = 0.83$; $P < 0.0001$). Although this recruitment scheme persisted and significant exponential relationships ($r > 0.65$; $P < 0.001$) were still found in the experimental groups after nerve crushing (Fig. 8*B* and *C*), their distributions shifted to the right (towards higher thresholds; Fig. 8*C*). Likewise threshold distribution, spacing (separation between successive thresholds) and recruitment gain (number of units recruited per $ET_{CO_2}$ change; Fig. 8*E*) were significantly altered after nerve lesions. Although almost 50% of control motoneurones (lower-threshold units) would already be firing at $ET_{CO_2} = 0\%$, these were recruited in a ranking extending down to $-50\%$ of $ET_{CO_2}$ while the remaining 50% of the sampled pool (higher-threshold units) would be recruited within only a 5% range of $ET_{CO_2}$ (Fig. 8*D*). As expected from the persistence of exponential relationships between threshold and $S_{mFR}$ after crushing, reductions in firing sensitivities were also accompanied by decreases in the recruitment thresholds (Fig. 8*B* and *C*). Cumulative histograms of recruitment thresholds showed that at 0% of $ET_{CO_2}$ the proportion of recruited motoneurones in the lesioned group was higher than in the control group (71.8% *versus* 48.7%; Fig. 8*D*). However, linearization of the exponential curves illustrated in Fig. 8*D* showed that above 0% of $ET_{CO_2}$ the recruitment gain, i.e. the recruitment rate by $ET_{CO_2}$ variation, was reduced in the crushed group relative to control (Fig. 8*E*).

To evaluate to what extent changes in recruitment properties and rate modulation could contribute to depressing the electrical activity in the HN after nerve lesion, we calculated the whole nucleus firing activity according to experimental data obtained from the control, lesioned (at 7 and 15 days after crushing) and recovered (at 30 days after crushing) motor pools along the 0–5% $ET_{CO_2}$ interval (Fig. 8; see legend). Predicted curves showed that, despite the higher percentage of recruited units at 0% in the crushed groups (Fig. 8*F*), the discharge activity of experimental groups never exceeded that calculated in the control. Likewise, mean activities estimated at 7 and 15 days in the 4.5–5% interval were reduced by 57.1% and 60.0% compared with the control, respectively, which was in agreement with experimental observations. These results indicate that, in addition to firing rate modulation, recruitment properties were altered by nerve lesion in the HN. However, although changes in threshold distributions led to a higher proportion of early recruited units in the crushed groups, this was not sufficient to compensate for reductions in firing rates and modulation.

© The Physiological Society 2004

### Changes in synaptophysin immunoreactivity in the HN

All the effects reported in relation to firing properties were long lasting. Changes appeared early during the first days, reached a plateau between days 7 and 15, and finally recovered over the third and fourth weeks. We further investigated whether changes in firing properties were accompanied by parallel morphological alterations affecting the density of synaptic boutons. To investigate this hypothesis we carried out immunostaining against synaptophysin, a marker of synaptic terminals. Optical density of immunolabelling in the hypoglossal neuropil was measured at different time points after nerve crushing. Synaptophysin immunolabelling was more dense in the HN than in the surrounding reticular formation (Fig. 9*A*–*D*) and appeared as a punctate-like staining when visualized at high magnification (Fig. 9*E* and *F*). No significant differences in the optical density between the two sides were observed at 1 day after nerve crushing (Figs 9*A* and *B*, and 10). However, at 7 and 15 days after injury, the optical density of synaptophysin immunoreactivity was reduced by $17.1 \pm 2.7\%$ and $21.0 \pm 5.4\%$ in the experimental side compared with the control side (Figs 9*C*–*F* and 10). Synaptic density in the crushed side was similar to the control side at 1 month after injury (Fig. 10). Inspection of the

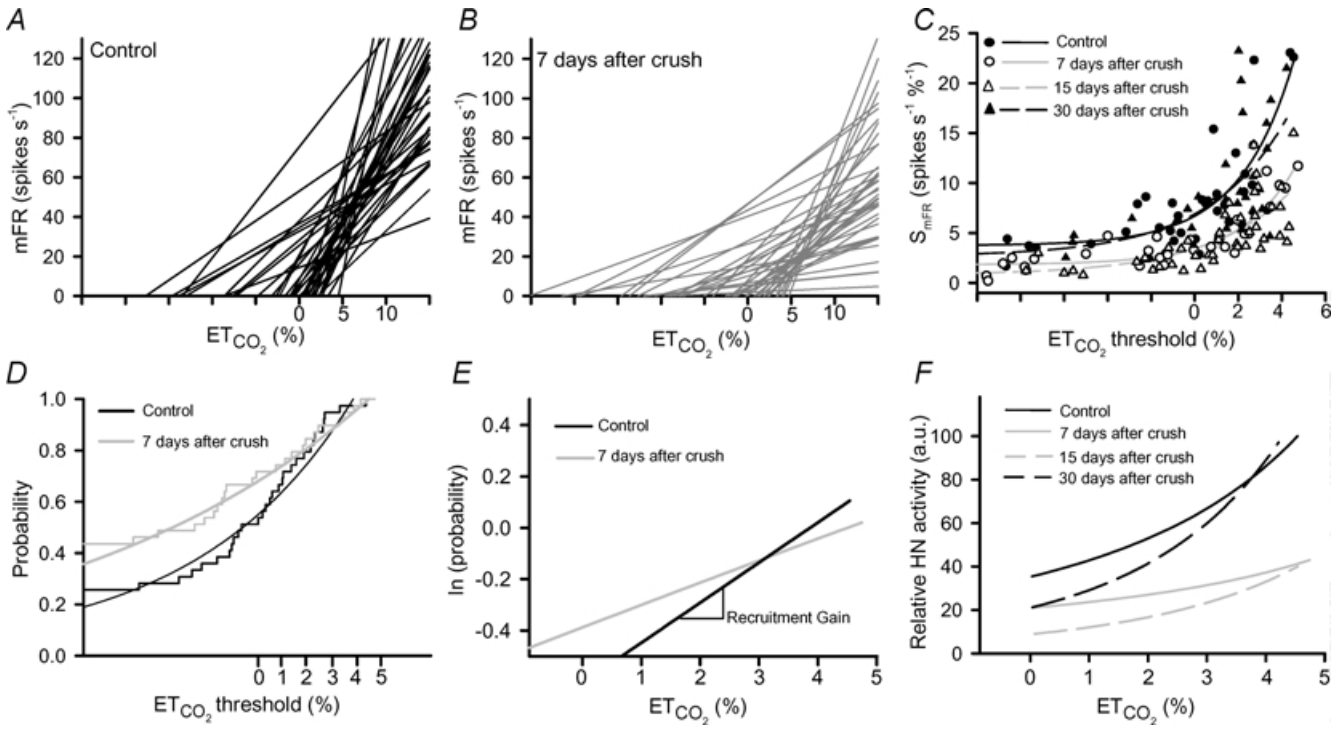


**Figure 8. Effects of XIIth nerve crushing on recruitment of hypoglossal motoneurones**
*A* and *B*, collection of linear regression lines of mean firing rate (mFR) *versus* $ET_{CO_2}$ including the whole analysed pools in control (*A*) and at 7 days after crushing (*B*). The abscissa intercept for each line indicates the theoretical recruitment threshold. *C*, plots reflecting the relationships between $S_{mFR}$ values (in spikes $s^{-1}$ $\%^{-1}$) and the recruitment thresholds for the motoneuronal groups sampled in the control and at 7, 15 and 30 days after crushing. Data point distributions were best fitted by exponential functions ($P < 0.0001$) whose regression curves were: $y = 3.75 + 2.95\exp(0.40x)$ ($r = 0.83$), $y = 1.83 + 1.63\exp(0.38x)$ ($r = 0.92$), $y = 0.81 + 2.63\exp(0.26x)$ ($r = 0.72$), and $y = 2.66 + 4.23\exp(0.28x)$ ($r = 0.66$) for the control and 7, 15 and 30 days post-injury groups, respectively. *D*, cumulative sum histograms of the recruitment thresholds obtained in control and at 7 days after crushing. Histograms were fitted by exponential growing functions ($P < 0.0001$) with equations $y = 0.01 + 0.53\exp(0.16x)$ ($r = 0.98$) and $y = -0.08 + 0.76\exp(0.07x)$ ($r = 0.99$) for the control and experimental data, respectively. *E*, graph showing the recruitment gain (as the line slopes) between 0 and 5% of $ET_{CO_2}$ for the neuronal pools illustrated in *D*. Linearization was obtained following semilogarithmic transformation of the ordinate axis scale. *F*, total spike activity (in arbitrary units) in the control and experimental hypoglossal nuclei (HNs). Motor output for each group was estimated as the product of the exponential curves in *D* (cumulative frequency of recruited units) times the cumulative mean $S_{mFR}$ in steps of 0.1% $ET_{CO_2}$ variations. For comparison, data were expressed relative to maximum output activity in the control situation.

© The Physiological Society 2004

immunostained material at higher magnification demonstrated a reduction in synaptophysin-immunoreactive terminals in the surrounding neuronal neuropil 2 weeks after nerve injury (Fig. 9*E* and *F*). These observations indicate that crushing the XIIth nerve induced a decrease in the number of synaptic terminals in the HN that was recovered with muscle re-innervation.

## Discussion

In this work we demonstrate that motor nerve lesion depresses the inspiratory activity of HMNs under basal conditions and during modulated respiratory drive produced by $ET_{CO_2}$ changes. Nerve crush also altered the pattern of HMN recruitment, increasing the proportion of low-threshold motoneurones. We conclude that functional alterations were due to a reduction in the efficacy of the synaptic inputs to HMNs, which in turn reflects, at least in part, a decrease in afferent terminals as suggested by the reduction of synaptophysin immunoreactivity following the lesion. Peripheral alterations were also reported including reductions in axonal conduction velocities and excitability. Changes in motor activity and axonal properties reverted in one month, when complete muscle re-innervation was achieved, as determined by the return of the full-amplitude CMAP. The results suggest that functional neuromuscular re-connection and the consequent establishment of trophic interactions are required for the recovery of normal electrical and synaptic properties of adult axotomized motoneurones. Our experimental approach, in which the level of an identified, physiological motor input to the motoneurone can be controlled in a repeatable manner simply by adjusting levels of $ET_{CO_2}$ and the chemoreceptor drive to the respiratory network, should prove useful in studying mechanisms underlying degenerative, regenerative and

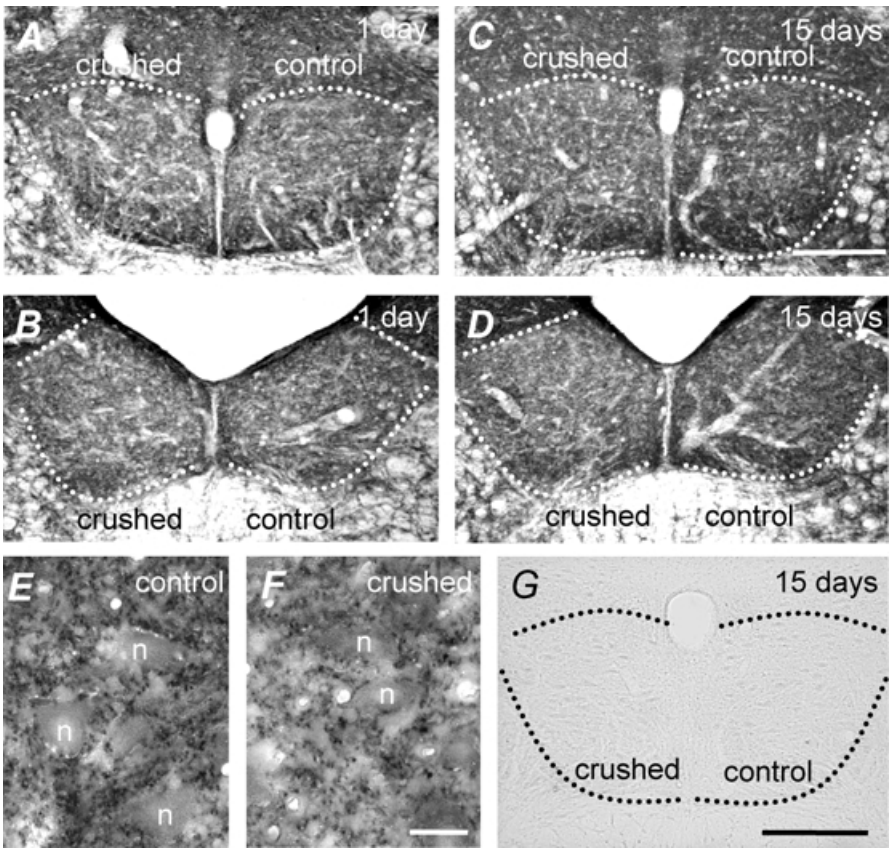


**Figure 9. Effects of XIIth nerve crushing on synaptic density in the hypoglossal nucleus**
*A–D*, photomicrographs obtained from coronal sections at different rostrocaudal levels in animals at 1 and 15 days post-lesion. In each section, the experimental side (crushed) was compared with the control side. *E* and *F*, high magnification photomicrographs showing neurones (n) surrounded by punctate-like synaptophysin immunoreactivity in the control (*E*) and crushed (*F*) sides, obtained 15 days after crushing. *G*, photomicrograph obtained from a coronal section of an animal 15 days post-lesion at a rostrocaudal level similar to that shown in *A* and *C*, in which primary antibody was omitted. Calibration bars: *A–D* and *G*, 250 $\mu$m; *E* and *F*, 25 $\mu$m.

© The Physiological Society 2004

synaptogenic phenomena in the central nervous system of adult mammals.

### Remarks about the methodological approach

Although significant efforts have been made to study membrane and synaptic responses to motor nerve axotomy, little is known about how these alterations affect responses of motoneurones to physiological inputs. Chronic studies in the spinal motor system have shown a reversible decline in motoneurone activity during locomotion following axotomy of several mixed nerves (Gordon *et al.* 1980). A major disadvantage in the interpretation of previous results is that loss of proprioceptive signals on the lesioned side would contribute to a reduced homonymous motor pool activity. In our experimental approach, where animals were vagotomized, decerebrated and a neuromuscular blocking agent administered, it would be expected that pulmonary, descending and proprioceptive afferents were similarly suppressed in control and lesioned sides. Eliminating the influence of these afferent sources that could be directly unbalanced by peripheral lesions and restricting the modalities of afferent information would permit more unambiguous interpretations.

Since most previous studies on the effects of muscle disconnection on motoneurones have used complete nerve transection, it is important to stress distinctions between different forms of nerve lesion. Regenerative and survival capacities could be differentially compromised in adult motoneurones following transection or avulsion of the peripheral nerve (Li *et al.* 1998). Crushing lesion causes complete axotomy but, unlike nerve transection, it preserves the endoneural tube, providing neurotrophic support and a physical guide for the proximal axonal ends (De Medinaceli, 1988). Consequently, motor nerve crush involves a shorter delay in achieving muscle re-innervation without significant neuronal loss (Rende *et al.* 1995; Tanaka *et al.* 1998). According to our observations, crushing the XIIth nerve immediately induced a complete suppression of CMAP, which was fully restored 30 days later in parallel with the integrated burst area of neurographic recordings. The complete recovery of these parameters one month after injury probably reflects that the number of functional motor units in both control and re-innervated conditions is similar. Therefore, the reduced nerve activity we observed after nerve lesion would be determined by functional axonal and central alterations without neuronal loss.

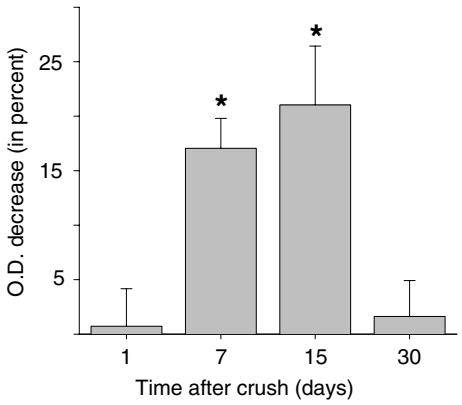


**Figure 10. Quantitative effects of XIIth nerve crushing on synaptic density in the hypoglossal nucleus**
Decrease of the optical density (O.D) in the experimental side compared to control side at the indicated time points after crushing. Values are means ± S.E.M. from 3 animals. *Significant differences ($P < 0.05$, non-parametric Mann-Whitney $U$ test) relative to measurements obtained at 1 day post-lesion.

### Peripheral response to XIIth nerve crushing

Following the XIIth nerve crushing, we found peripheral electrophysiological alterations that appeared on the proximal motor axons and dennervated muscle. The slowed proximal impulse conduction and the increased threshold to evoke antidromic spikes have been also reported in peripheral and sensory myelinated fibres after nerve transection (Milner & Stein, 1981; Foehring *et al.* 1986). Several factors have been suggested as underlying these axonal disturbances, such as decreases in the thickness of the myelin sheaths and the axonal diameter (Hoffman *et al.* 1987; Titmus & Faber, 1990). The distribution of antidromic latencies was progressively widened and skewed to longer values from 3 to 15 days post-injury. This latter time point coincided with initial phases of muscle re-innervation as indicated by the re-appearance of CMAPs. The fact that they were reduced in amplitude and polyphasic probably reflects increased asynchrony in the arrival of motor impulses. Thereafter, antidromic latency returned to normal in parallel with most of the CMAP parameters, which is in agreement with a target-derived trophic control of axonal properties.

Despite proximal recovery at 30 days, CMAP latency remained slightly longer than the control, perhaps due to an incomplete recovery in fibre size, myelinization or both, in regenerated distal axons. It has been suggested that functional and structural axonal properties of fast conducting units (with greater axon calibre) would be preferentially affected over slow units following motor or sensory nerve axotomy (Milner & Stein, 1981; Titmus &

© The Physiological Society 2004

Faber, 1990). Consequently, a larger and faster decline in fibre size and conduction velocity and a longer delay in recovery would be expected in large myelinated motor fibres (Titmus & Faber, 1990). The longer latency observed one month after XIIth nerve crushing could indicate a partial prevalence of the structural and functional effects on faster motor units.

### Depression in firing activity of HMNs following XIIth nerve crushing

The main alterations observed in the firing pattern of HMNs following XIIth nerve crushing were an overall reduction in firing rates and an almost complete loss of modulation by chemosensory afferents. Factors contributing to these alterations could include changes either in pre-motor afferent activity, in motoneurone excitability and/or in the strength of the synaptic inputs to motoneurones. Modifications of central respiratory patterns induced by peripheral crushing are discounted since (1) although mechanosensory afferent signals could differentially modulate respiratory output in crushed *versus* intact pools, these peripheral inputs were mostly and similarly reduced in both; (2) although permanent motor or sensory deprivation can induce changes in the activity and topography of higher order central structures (Kaas *et al.* 1999; Chen *et al.* 2002), such extension for axotomy-induced retrograde effects has never been reported following reversible peripheral nerve lesions; and (3) the modulation in BR and DB by $ET_{CO_2}$ changes remained similar in control and lesioned animals, suggesting that pre-motor responsiveness was largely preserved.

Membrane excitability is up-regulated in hypoglossal and spinal motoneurones (Eccles *et al.* 1958; Kuno & Llinás, 1970*a*,*b*; Gustaffson, 1979; Takata *et al.* 1980) following axotomy. Accordingly, it could be expected that membrane alterations would make axotomized HMNs more responsive to synaptic inputs. However, our results appeared to indicate reduced sensitivity to afferent drive. Therefore, although membrane alterations could contribute to the modification of some functional properties such as recruitment distribution (see below), they are not likely to underlie the changes in discharge activity and modulation shown here. As suggested by parallel reductions in synaptophysin immunolabelling, these firing alterations would be better explained by loss of afferent signals.

In relation to the present results, previous studies have revealed that firing sensitivity to afferent signals could be linked to the degree of afferent synaptic innervation (Moreno-López *et al.* 1997; González-Forero *et al.* 2002, 2003). Likewise, axotomized motoneurones show attenuated synaptic potentials that have been associated with massive synaptic stripping (Kuno & Llinás, 1970*b*; Brännström & Kellerth, 1998). Such synaptic detachment may differentially affect excitatory and inhibitory terminals. In HMNs, axotomy mainly affects S-type boutons, forming excitatory synapses (Sumner, 1975). Because the inspiratory-related discharge in HMNs is determined by afferent synaptic excitation (Ono *et al.* 1994; Peever *et al.* 2002), and since that firing activity was reduced in experimental animals, we might conclude that excitatory synaptic transmission was depressed by lesion of the XIIth nerve.

### Changes in recruitment scheme and motor output after XIIth nerve crushing

The output of a motor pool is regulated by both recruitment gradation and firing rate modulation. Since thresholds, firing rate gains, force production and, frequently, synaptic strengths vary for each unit in a motor pool, one would expect a certain degree of covariation between these variables in order to adjust force production to motor requirements. Although recruitment order is primarily determined by the size principle (Henneman *et al.* 1965; Gustaffson & Pinter, 1985), the organization of synaptic inputs could ultimately determine the rank and gain for recruitment or even facilitate disruption of the size-determined scheme (Kernell & Hultborn, 1990; Heckman & Binder, 1993). According to the size principle, slower conducting phrenic motoneurones are recruited first during inspiration (Jodkowski *et al.* 1987). For HMNs this information is lacking, although it has been suggested that the recruitment pattern of this pool differs from that of phrenic units (Hwang *et al.* 1983*a*). In our study, no information about size-related parameters other than unitary antidromic latency could be obtained. However, we did not find good relationships ($r < 0.5$) between latency and threshold.

On the other hand, recruitment thresholds were exponentially correlated with $S_{mFR}$. Motoneurones with lower $S_{mFR}$ were usually recruited earlier than those with higher gains. This recruitment scheme was not altered by XIIth nerve lesions, indicating that $S_{mFR}$ were good predictors of the recruitment sequence in both control and experimental HNs. Similar relationships between firing rate gains and threshold have been found in cat abducens motoneurones (Pastor & González-Forero, 2003) and would be expected from the work of Monster & Chan (1977) on human spinal motoneurones. Therefore,

© The Physiological Society 2004

such distributions could represent a common principle for recruitment organization in motor pools. Likewise, the rate of recruitment (recruitment gain) increased with thresholds in parallel with firing rate gains. A non-homogeneous distribution of thresholds and $S_{mFR}$ over the motor range could be related to requirements for a gradation of force production. The poor firing rate modulation and reduced recruitment gain for low threshold units would be more suitable for sustaining a repetitive inspiratory discharge at low levels of force output. Since for these earlier recruited units, thresholds usually fell outside the 0–5% $ET_{CO_2}$ range, a minimal basal inspiratory activation would be always guaranteed in physiological conditions. This can be critical for maintaining upper airways patency during low activity states such as sleep. The absence of these always-active units could be associated with the symptomatic presence of the obstructive sleep apnoea syndrome. In contrast, a higher firing rate and recruitment gains beyond 0% of $ET_{CO_2}$ would make the motor pool more responsive to changes in afferent drive in physiological conditions. Therefore, the distribution of recruitment and rate gradations over the motor range would facilitate appropriate force modulation between 0 and 5% of $ET_{CO_2}$ superimposed on a minimal basal activation.

Since nerve lesion affects both intrinsic (membrane properties) and extrinsic (synaptic organization) properties, the recruitment alterations reported here would be complex to interpret. The elevation of input resistance and reduction of rheobase lead to a decrease in the current thresholds for impulse discharge in axotomized motoneurones (Gustaffson, 1979). On the other hand, synaptic input loss could differentially affect recruitment properties depending on afferent distribution over the motoneurone pool (Kernell & Hultborn, 1990; Heckman & Binder, 1993). We found that XIIth nerve lesion led to a higher proportion of low-sensitivity and early recruited units as well as to reductions in the recruitment gain across the physiological range. Therefore, it is possible that the recruitment alterations noticed here result from both increased excitability and loss of afferent signals. Increased input resistance could explain an elevated incidence of low threshold units, while changes in the recruitment gain would be better related to the reorganization of synaptic inputs. This suggestion is in agreement with present findings and previous reports on spinal and cranial motoneurones showing changes in the recruitment gain following selective or massive deafferentation (Powers & Rymer, 1988; Haftel *et al.* 2001; Pastor & González-Forero, 2003). After XIIth nerve crushing, a reduction in the recruitment gain could be associated with the loss of efficacy from inspiratory afferent inputs that scale in parallel to firing rate gains in the HMN pool, i.e. inducing higher synaptic responses in motoneurones with high sensitivities and thresholds. Alternatively, as noticed above, it is also possible that XIIth nerve lesions induce more profound functional and anatomical alterations in high threshold motoneurones (Milner & Stein, 1981; Giannini *et al.* 1989; Titmus & Faber, 1990). Hence, a more specific effect of XIIth nerve crushing on high-threshold HMNs, implying greater membrane and synaptic alterations, could contribute to reducing the proportion of motoneurones recruited in the 0–5% $ET_{CO_2}$ interval, and to increasing the number of those with lower thresholds and sensitivities.

As indicated by experimental and predicted data, an earlier recruitment was not associated with higher motor output in the lesioned HMN pool. Total firing activity in the experimental nucleus never exceeded that of the control pool. That would be obvious since the relationships between thresholds and $S_{mFR}$ persisted after crushing, and therefore the reduction of thresholds was also associated with gain decreases. These data indicate that alterations in the recruitment distribution did not contribute to the depression of electrical activity in the HN. We conclude that the deficient firing rate modulation in the HN is the primary cause of activity depression after peripheral nerve lesion.

### Opposition between membrane and synaptic alterations following target disconnection. Compensatory response or functional de-differentiation?

A generalized finding for axotomized motoneurones is the increased membrane excitability (Titmus & Faber, 1990; González-Forero *et al.* 2004). Electrical changes implicate reductions in the rheobase and increases in the membrane time constant, input resistance and gain for the ratio between firing rate and current intensity (Heyer & Llinás, 1977; Gustaffson, 1979; Takata *et al.* 1980). Consequently, electrical changes would be expected to facilitate firing activity in response to synaptic inputs and reduce the threshold for discharge. However, despite this presumed facilitation, axotomized motoneurones usually show attenuated synaptic responses (Eccles *et al.* 1958; Kuno & Llinás, 1970*b*) and as reported here, have depressed firing activity, and do not respond to enhanced synaptic (chemoreceptor) drive. Therefore, we suggest that, under physiological patterns of activation, the effects of deafferentation prevail over those arising from membrane alterations in axotomized HMNs.

© The Physiological Society 2004

The functional significance of these obviously counterposed changes remains uncertain, although some authors have suggested that electrical alterations would imply a functional de-differentiation in axotomized motoneurones towards a postnatal-like stage (Kuno *et al.* 1974). Anatomical and electrical properties of neonatal motoneurones mature in parallel with muscle fibres after motor axons reach their target muscles (Navarrette & Vrbova, 1993). Therefore, the activation of regrowth programmes in adult motor axons following axotomy could require reversion towards an immature electrical phenotype. Another possibility is that increased excitability in axotomized motoneurones would constitute a compensatory response to counteract the deficiency in ongoing excitatory drive (Eccles *et al.* 1958: Kuno & Llinás, 1970*a*). In lesioned HMNs, reductions in firing activity and modulation were not completely compensated by possible membrane alterations since they persisted during muscle disconnection and recovered when neuromuscular transmission was restored. However, increased membrane excitability could sustain certain levels of electrical activity necessary to prevent atrophy or neuronal death, and favour axonal growth, synaptogenesis and differentiation in both immature and regenerating motoneurones.

### Implications for nerve regeneration and functional recovery

Motor unit differentiation during development is modulated by patterns of electrical activity (Kalb & Hockfield, 1992; Navarrette & Vrbova, 1993). Because axotomized motoneurones exhibit electrical, histochemical and anatomical properties that resemble those observed in neonatal motoneurones (Kuno *et al.* 1974), it is possible that the differential patterns of electrical activity shown by regenerating motoneurones, at least to a certain degree, play a role in instructing axonal regrowth and target re-innervation. Chronic electrical stimulation increases the speed and accuracy of motor axon regeneration following peripheral nerve transection in adulthood (Al-Majed *et al.* 2000). Therefore, we can speculate that reduced afferent synaptic and firing activity in HMNs after XIIth nerve lesions would condition a low rate of regeneration. Additionally, firing depression in the HMN pool could also contribute to the loss of specificity during regeneration that usually leads to aberrant muscle re-innervation and anomalous contraction patterns (Mizuno *et al.* 1980; Wilson *et al.* 1994). Our findings could be used as a reference for developing therapeutic approaches that compensate discharge depression after peripheral nerve injury. It remains to be determined if, as has been demonstrated for the effect of electrical stimulation, treatments that increase afferent synaptic drive and firing activity in motoneurones would promote a faster and more appropriate muscle re-innervation.

The findings reported here contribute to a better understanding of the physiological alterations derived from physical disconnection between motoneurones and muscle. We have demonstrated that lesion of the XIIth nerve led to reduced firing activity in the HN that, in combination with the marked reduction in synaptic inputs, resulted in a poor motor output across the whole motor range. Previous studies have reported similar reductions in the spontaneous activity displayed by sensory and motor neurones (Gordon *et al.* 1980; Delgado-García *et al.* 1988; Seburn *et al.* 1999). In conclusion, the decline in firing activity caused by the loss or reduction of afferent drive appears to constitute a common response to target disconnection for different neuronal populations.

## References

Al-Majed AA, Neumann CM, Brushart TM & Gordon T (2000). Brief electrical stimulation promotes the speed and accuracy of motor axonal regeneration. *J Neurosci* **20**, 2602–2608.

Brännström T & Kellerth JO (1998). Changes in synaptology of adult cat spinal $\alpha$-motoneurons after axotomy. *Exp Brain Res* **118**, 1–13.

Brushart TM, Hoffman PN, Royall RM, Murinson BB, Witzel C & Gordon T (2002). Electrical stimulation promotes motoneuron regeneration without increasing its speed or conditioning the neuron. *J Neurosci* **22**, 6631–6638.

Chen R, Cohen LG & Hallett M (2002). Nervous system reorganization following injury. *Neuroscience* **111**, 761–773.

Cohen MI (1968). Discharge patterns of brain-stem respiratory neurons in relation to carbon dioxide tension. *J Neurophysiol* **31**, 142–165.

De Medinaceli L (1988). Functional consequences of experimental nerve lesions: effects of reinnervation blend. *Exp Neurol* **100**, 166–178.

Delgado-García JM, Del Pozo F & Baker R (1988). Behavior of neurons in the abducens nucleus of the alert cat – III. Axotomized motoneurons. *Neuroscience* **24**, 143–160.

Eccles JC, Libet B & Young RR (1958). The behavior of chromatolysed motoneurons studied by intracellular recording. *J Physiol* **143**, 11–40.

Foehring RC, Sypert GW & Munson JB (1986). Properties of self-reinnervated motor units of medial gastrocnemius of cat. II. Axotomized motoneurons and time course of recovery. *J Neurophysiol* **55**, 947–965.

© The Physiological Society 2004

Foehring RC, Sypert GW & Munson JB (1987*a*). Motor unit properties following cross-reinnervation of cat lateral gastrocnemius and soleus muscles with medial gastrocnemius nerve. I. Influence of motoneurons on muscle. *J Neurophysiol* **57**, 1210–1226.

Foehring RC, Sypert GW & Munson JB (1987*b*). Motor unit properties following cross-reinnervation of cat lateral gastrocnemius and soleus muscles with medial gastrocnemius nerve. II. Influence of muscle on motoneurons. *J Neurophysiol* **57**, 1227–1245.

Giannini C, Lais AC & Dyck PG (1989). Number, size and class of peripheral nerve fibers regenerating after crush, multiple crush, and graft. *Brain Res* **500**, 131–138.

González-Forero D, Álvarez FJ, de la Cruz RR, Delgado-García JM & Pastor AM (2002). Influence of afferent synaptic innervation on the discharge variability of cat abducens motoneurones. *J Physiol* **541**, 283–299.

González-Forero D, Benítez-Temiño B, de la Cruz RR & Pastor AM (2004). Functional recovery in the peripheral and central nervous system after injury. In *Brain Damage and Repair. From Molecular Reseach to Clinical Therapy*, ed. Herdegen T & Delgado-García JM pp. 285–305. Kluwer Academic Publishers, Durdrecht.

González-Forero D, de la Cruz RR, Delgado-García JM, Álvarez FJ & Pastor AM (2003). Functional alterations of cat abducens neurons after peripheral tetanus neurotoxin injection. *J Neurophysiol* **89**, 1878–1890.

Gordon T, Hoffer JA, Jhamandas J & Stein RB (1980). Long-term effects of axotomy on neural activity during cat locomotion. *J Physiol* **303**, 243–263.

Gustaffson B (1979). Changes in motoneurone electrical properties following axotomy. *J Physiol* **293**, 197–215.

Gustaffson B & Pinter MJ (1985). On factors determining orderly recruitment of motor units: a role for intrinsic membrane intrinsic properties. *Trends Neurosci* **8**, 431–433.

Haftel VK, Prather JF, Heckman CJ & Cope TC (2001). Recruitment of cat motoneurons in the absence of homonymous afferent feedback. *J Neurophysiol* **86**, 616–628.

Heckman CJ & Binder MD (1993). Computer simulations of the effects of different synaptic input systems on motor unit recruitment. *J Neurophysiol* **70**, 1827–1840.

Henneman E, Somjen G & Carpenter DO (1965). Functional significance of cell size in spinal motoneurons. *J Neurophysiol* **28**, 560–580.

Heyer CB & Llinás R (1977). Control of rhythmic firing in normal and axotomized cat spinal motoneurons. *J Neurophysiol* **40**, 480–488.

Hoffman PN, Cleveland PW, Griffin JW, Landes PW, Cowan NJ & Price DL (1987). Neurofilament gene expression: a major determinant of axonal caliber. *Proc Natl Acad Sci USA* **84**, 3472–3476.

Hwang JC, Bartlett D Jr & St John WM (1983*a*). Characterization of respiratory-modulated activities of hypoglossal motoneurons. *J Appl Physiol* **55**, 793–798.

Hwang JC, St John WM & Bartlett D Jr (1983*b*). Respiratory-related hypoglossal nerve activity: influence of anesthetics. *J Appl Physiol* **55**, 785–792.

Jodkowski JS, Viana F, Dick TE & Berger AJ (1987). Electrical properties of phrenic motoneurons in the cat: correlation with inspiratory drive. *J Neurophysiol* **58**, 105–124.

Kaas JH, Florence SL & Jain N (1999). Subcortical contributions to massive cortical reorganizations. *Neuron* **22**, 657–660.

Kalb RG & Hockfield S (1992). Activity dependent development of spinal cord motor neurons. *Brain Res Brain Res Rev* **17**, 283–289.

Kernell D & Hultborn H (1990). Synaptic effects on recruitment gain: a mechanism of importance for the input-output relations of motoneurone pools. *Brain Res* **507**, 176–179.

Kuno M & Llinás R (1970*a*). Enhancement of synaptic transmission by dendritic potentials in chromatolysed motoneurones of the cat. *J Physiol* **210**, 807–821.

Kuno M & Llinás R (1970*b*). Alterations of synaptic action in chromatolysed motoneurones of the cat. *J Physiol* **210**, 823–838.

Kuno M, Miyata Y & Muñoz-Martínez EJ (1974). Differential reaction of fast and slow $\alpha$-motoneurones to axotomy. *J Physiol* **240**, 725–739.

Li L, Houenou LJ, Wu W, Lei M, Prevette DM & Oppenheim RW (1998). Characterization of spinal motoneuron degeneration following different types of peripheral nerve injury in neonatal and adult mice. *J Comp Neurol* **396**, 158–168.

Mendell LM (1984). Modifiability of spinal synapses. *Physiol Rev* **64**, 260–324.

Milner TE & Stein RB (1981). The effects of axotomy on the conduction of action potentials in peripheral sensory and motor nerve fibres. *J Neurol Neurosurg Psychiatry* **44**, 485–496.

Mizuno N, Uemura-Sumi N, Matsuda K, Takeuchi Y, Kume M & Matsushima R (1980). Non-selective distribution of hypoglossal nerve fibers after section and resuture: a horseradish peroxidase study in the cat. *Neurosci Lett* **19**, 33–37.

Monster AW & Chan H (1977). Isometric force production by motor units of extensor digitorum communis muscle in man. *J Neurophysiol* **40**, 1432–1443.

Moreno-López B, de la Cruz RR, Pastor AM & Delgado-García JM (1997). Effects of botulinum neurotoxin type A on abducens motoneurons in the cat: alterations of the discharge pattern. *Neuroscience* **81**, 437–455.

Navarrette R & Vrbova G (1993). Activity-dependent interactions between motoneurones and muscles: their role in the development of the motor unit. *Prog Neurobiol* **41**, 93–124.

Ono T, Ishiwata Y, Inaba N, Kuroda T & Nakamura Y (1994). Hypoglossal premotor neurons with rhythmical inspiratory-related activity in the cat: localization and projection to the phrenic nucleus. *Exp Brain Res* **98**, 1–12.

© The Physiological Society 2004

Pastor AM & González-Forero D (2003). Recruitment order of cat abducens motoneurons and internuclear neurons. *J Neurophysiol* **90**, 2240–2252.

Peever JH, Shen L & Duffin J (2002). Respiratory pre-motor control of hypoglossal motoneurons in the rat. *Neuroscience* **110**, 711–722.

Powers RK & Rymer WZ (1988). Effects of acute dorsal spinal hemisection on motoneuron discharge in the medial gastrocnemius of the decerebrate cat. *J Neurophysiol* **59**, 1540–1556.

Rende M, Giambanco I, Buratta M & Tonali P (1995). Axotomy induces a different modulation of both low-affinity nerve growth factor receptor and choline acetyltransferase between adult rat spinal and brainstem motoneurons. *J Comp Neurol* **363**, 249–263.

Sawczuk A & Mosier KM (2001). Neural control of tongue movements with respect to respiration and swallowing. *Crit Rev Oral Biol Med* **12**, 18–37.

Seburn KL, Catlin PA, Dixon JF, Lee MH, Matteson MS & Cope TC (1999). Decline in spontaneous activity of group alpha-beta sensory afferents after sciatic nerve axotomy in rat. *Neurosci Lett* **274**, 41–44.

Sumner BEH (1975). A quantitative analysis of boutons with different types of synapse in normal and injured hypoglossal nuclei. *Exp Neurol* **49**, 406–417.

Takata M & Nagahama T (1984). Cortically induced postsynaptic potentials in hypoglossal motoneurons after axotomy. *Neuroscience* **13**, 855–862.

Takata M, Shohara E & Fujita S (1980). The excitability of hypoglossal motoneurons undergoing chromatolysis. *Neuroscience* **5**, 413–419.

Tanaka H, Kaneko K, Satoh H, Hiraba H, Ishibashi Y, Watabe K, Inage T & Kamogawa H (1998). Regenerative process after experimental injury of hypoglossal nerves in guinea pigs. *J Oral Sci* **40**, 147–152.

Titmus MJ & Faber DS (1990). Axotomy-induced alterations in the electrophysiological characteristics of neurons. *Prog Neurobiol* **35**, 1–51.

Wang SC & Nims LF (1948). The effects of various anesthetics and decerebration on the $CO_2$ stimulating action on respiration in cats. *J Pharmacol Exp Ther* **92**, 187–195.

Wilson JR, Sumner AJ & Eichelman J (1994). Aberrant innervation following hypoglossal nerve damage. *Muscle Nerve* **17**, 931–935.

## Acknowledgements

We would like to thank Dr C. Estrada for a critical reading of the manuscript. This work was supported by a grant from the Ministerio de Ciencia y Tecnología (BFI2001-3186). D.G.-F. was supported by a grant from the Junta de Andalucía (PAI/COORD-GR/PR/2001-052), Spain.

## Author's present address

D. González-Forero: Department of Anatomy and Physiology, Wright State University, Dayton, OH 45435, USA.

© The Physiological Society 2004